IS-T 1701

Studies of Selenium and Xenon in Inductively Coupled Plasma Mass Spectrometry

by

Bricker, Tonya

MS Thesis submitted to Iowa State University

Ames Laboratory, U.S. DOE

Iowa State University

Ames, Iowa 50011

Date Transmitted: July 27, 1994

PREPARED FOR THE U.S. DEPARTMENT OF ENERGY

UNDER CONTRACT NO. W-7405-Eng-82.

DISCLAIMER

DISCLAIMER

Portions of this document may be illegible in electronic image products. Images are produced from the best available original document.

TABLE OF CONTENTS

GENERAL INTRODUCTION

Since its development, inductively coupled plasma mass spectrometry (ICP-MS) has been a widely used analytical technique (1). ICP-MS offers low detection limits, easy determination of isotope ratios, and simple mass spectra from analyte elements. ICP-MS has been successfully employed for many applications including geological, environmental, biological, metallurgical, food, medical, and industrial (2-42). One specific application important to many areas of study involves elemental speciation by using ICP-MS as an element specific detector interfaced to liquid chromatography (43-74). Elemental speciation information is important and cannot be obtained by atomic spectrometric methods alone which measure only the total concentration of the element present. Part I of this study describes the speciation of selenium in human serum by size exclusion chromatography (SEC) and detection by ICP-MS.

Although ICP-MS has been widely used, room for improvement still exists. Difficulties in ICP-MS include noise in the background, matrix effects, clogging of the sampling orifice with deposited solids, and spectral interference caused by polyatomic ions. Previous work has shown that the addition of xenon into the central channel of the ICP decreases polyatomic ion levels (75). In Part II of this work, a fundamental study involving the measurement of the excitation temperature is carried out to further understand xenon's role in the reduction of polyatomic ions.

ICP-MS Overview

The inductively coupled plasma is an electrodeless discharge sustained by radio frequency power coupled through a load coil. The plasma is supported inside a torch made of concentric quartz tubes (see Figure 1). The sample is introduced as an aerosol

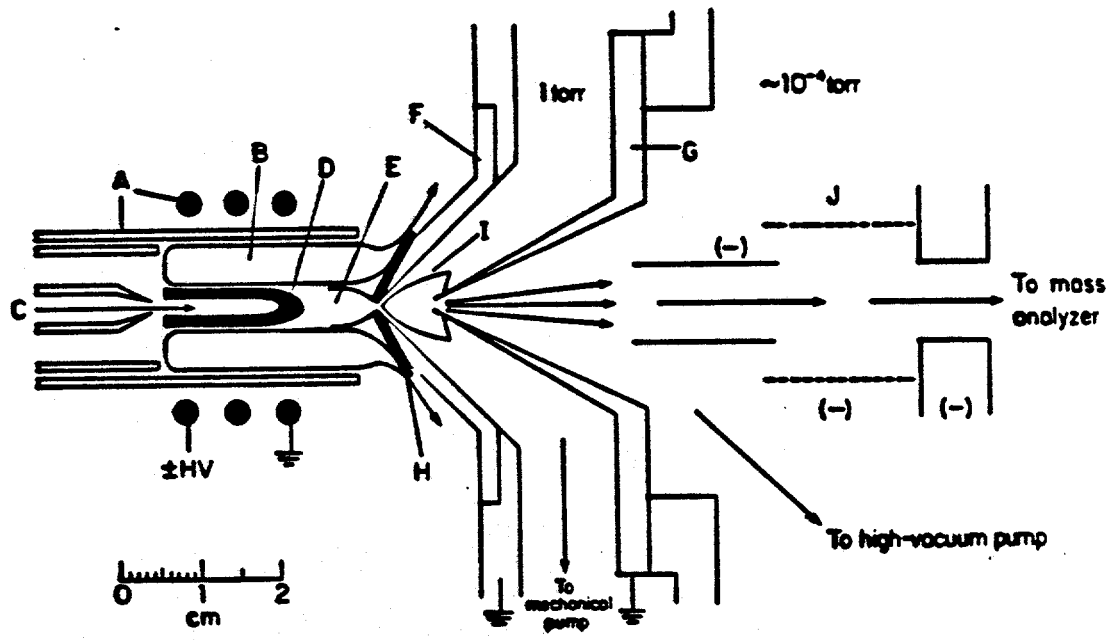

Figure 1. ICP and ion sampling interface. A = torch and load coil (HV = high voltage), B = induction region of ICP, C = a solution aerosol being injected into axial channel, D = initial radiation zone, E = normal analytical zone, F = nickel cone with sampling orifice in tip, G = skimmer cone, H = boundary layer of ICP gas deflected outside sampling orifice, I = expanding jet of C gas sampled from ICP, and J = ion lens elements. Reproduced from reference (76) with permission.

through the central tube in a flow of argon. The temperature of the ICP is in the range of 6000 K to 8000 K (77-78). This high temperature allows the introduced sample to be vaporized, atomized, and ionized. Most elements are ionized in the plasma with 100% efficiency (2). However, certain elements with high ionization energies are ionized to a lesser degree. For example, selenium has an ionization energy of 9.75 eV and is only 33% ionized in the plasma.

Due to the atmospheric pressure conditions in the plasma, the ions must be extracted into a vacuum system before mass analysis. Figure 1 shows the typical interface for the extraction of ions. The ions are sampled by a sampling orifice of about 1.0 mm diameter positioned in the normal analytical zone (see Figure 1). Ions and neutral gas flow into the first stage of the vacuum system where a supersonic jet is formed. The center portion of the jet flows through a second orifice called the skimmer. Behind the skimmer, several ion lenses focus the ions into a quadrupole mass analyzer (2).

For most ICP-MS experiments a conventional pneumatic nebulizer is used to introduce the liquid sample into the plasma. The liquid sample is introduced through a narrow tube and shattered into droplets at the end by interaction with a flow of argon gas. To avoid solvent overload of the plasma, a spray chamber is typically employed to remove the large droplets. With this type of nebulizer all but 1-3% of the sample is lost to the drain. When coupled to liquid chromatography, the spray chamber causes band broadening due to its large dead volume. For chromatographic separations, the direct injection nebulizer (DIN) is a more attractive sample introduction system for ICP-MS. The design and construction of the DIN have been described elsewhere (55, 79). The DIN is essentially composed of a fused silica capillary inside a ceramic support rod with a metal tip at its end. The liquid is introduced through the capillary while an argon gas flow is introduced into the ceramic rod allowing a spray of droplets to be created

pneumatically. The DIN is directly inserted inside the ICP torch and therefore all of the sample reaches the ICP.

PART I

SELENIUM SPECIATION BY SIZE EXCLUSION-INDUCTIVELY COUPLED PLASMA MASS SPECTROMETRY

INTRODUCTION

Trace element speciation is required for detailed information about the availability and mobility of an element in the environment and its behavior in biological and geochemical systems. Speciation studies require separation of the various chemical forms prior to determination of the element. Liquid chromatography (LC) has been coupled to inductively coupled plasma mass spectrometry (ICP-MS) to accomplish such experiments (77-105). Various modes of LC including reversed-phase (RP) (78-82), reversed-phase ion-pairing (RP-IP) (83-91), anion chromatography (AC) (78, 85, 92-95), cation chromatography (CC) (87, 96-97) and size exclusion chromatography (SEC) (78, 98-105) have been combined with ICP-MS. One example where speciation experiments are of interest is the study of selenium.

Selenium has been recognized as an essential nutrient since the 1950s (106-107). Deficiency of selenium has been associated with numerous disorders in animals. Keshan's disease, a cardiomyopathy affecting children and child-bearing women in China is selenium responsive. Selenium may also be connected with cirrhosis, cancer, and coronary heart disease. The two common inorganic forms of selenium, selenite SeO_3^{2-} and selenate SeO_4^{2-}, are considered to be toxic. Symptoms of selenium toxicity in animals include inflammation of the feet and softening and loss of hoofs and horns. In humans, loss of hair and nails and irritation of skin and eyes are caused by selenium toxicity. Selenium detoxification in the body occurs through metabolic conversion of selenite to the trimethylselenium ion which is excreted in urine (108-109).

Forms of selenium that occur in living organisms include the low-molecular-weight compounds, selenocysteine, selenohomocystine, selenomethionine, dimethylselenide, selenotaurine, and the enzymes glutathione peroxidase, formate reductase, and glycine reductase. In some bacteria, a seleno-transfer RNA is present (110). The nutritional value

of selenium and its absorption from the gastrointestinal tract vary with chemical form and the amount of the element ingested (111). Dietary forms of selenium include selenocysteine and selenomethionine. Fish and whole grains contain high levels of these selenium compounds. The availability of either total selenium or different forms of selenium in the diet and the amount of methionine consumed are only some of the factors that might contribute to the final distribution of selenium in specific selenoproteins (containing selenocysteine) or nonspecific selenoproteins (containing selenomethionine). After association with plasma proteins, selenium is delivered to all tissues including the bones, hair, the erythrocytes, and the leucocytes (112). Selenium is found at its highest concentration in the kidney, followed by the glandular tissues, including the pancreas, pituitary, and the liver. Many studies have tried to elucidate the incorporation of selenium into the selenoproteins (113). The major known fates of selenium in animals are incorporation into protein as selenocysteine, incorporation into certain modified tRNAs, and excretion as methylated compounds (113).

Two plasma selenoproteins, glutathione peroxidase and selenoprotein P, have been characterized. Glutathione peroxidase contains four identical subunits, each containing selenium in the form of a single selenocysteine residue. Selenoprotein P (plasma) is a glycoprotein secreted by the liver containing 7.5 ± 1 selenocysteines per molecule. The functions of these two plasma proteins are unknown. Glutathione peroxidase was considered an important antioxidant. However, the capacity of plasma glutathione peroxidase to remove H_2O_2 under physiological conditions can be questioned, which leaves open the possibility of other functions for this enzyme (113). Selenoprotein P may play a redox role, although evidence to support this is limited (114). Another proposed function for Selenoprotein P is the transport of selenium (115). More work is necessary to elucidate the roles of these selenoproteins.

The separation of metalloproteins in human serum has been accomplished by SEC-DIN-ICP-MS (116). Fassel and coworkers originally described the direct injection nebulizer (DIN) which is a microconcentric pneumatic nebulizer placed inside the ICP torch (117). In comparison to a conventional pneumatic nebulizer, the DIN allows reduced analyte memory effects, the elimination of sample transport losses and low dead volumes with quicker rinse out times and less peak broadening. These attributes make the DIN an attractive sample introduction system for liquid chromatography. In this study, the separation of metalloproteins was carried out by SEC while employing ICP-MS for the determination of selenium.

EXPERIMENTAL SECTION

HPLC-DIN-ICP-MS

A schematic diagram of the instrumental setup is shown in Figure 1. The HPLC system was composed of an SSI Model 222D metal-free microflow pump (Scientific Systems, Inc., State College, PA), a Rheodyne 9010 metal-free high-pressure sample injector with a 3 µl PEEK injection loop, and a 2.0-mm-i.d. x 25-cm-long size exclusion column (GPC 300, SynChrom, Inc., Lafayette IN). The outlet of the column was connected to the DIN through a switching valve (9010 Rheodyne) with a narrow bore polysil tube (50 µm-i.d. x 5-cm-long, Scientific Glass Engineering, Inc., Austin, TX). The narrow bore connecting capillary minimized extra column band broadening. A polysil tube was also used to connect the sample injector valve to the inlet of the column.

The design and construction of the DIN has been described elsewhere (74, 89). A 50-µm-i.d. x 40-cm-long fused silica capillary was used to transport the effluent from the column to the plasma. The 50 µm i.d. capillary is less susceptible to plugging with the high salt content in the matrix of human serum than the previous 30 µm i.d. capillary. The width of the annular gap between the inner capillary and the nebulizer tip was ≈25 µm.

The ICP-MS instrument used was the Elan Model 250 (Perkin-Elmer Sciex, Thornhill, ON, Canada). Instrument operating conditions were optimized to provide maximum ion signal for a 10 ppm Se standard solution (PlasmaChem Associates, Inc., Bradley Beach, NJ). The instrument operating parameters and chromatographic conditions are summarized in Tables I and II respectively.

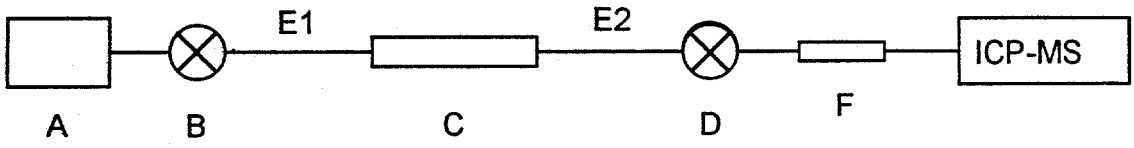

Figure 1. Schematic diagram of instrumental setup for the speciation of selenium in human serum with ICP-MS detection. A = HPLC pump, B = injection valve with 3 µl sample loop, C = analytical column, D = switching valve, E1, E2 = polysil connecting tubing, F = direct injection nebulizer (DIN).

Table I. Instrument Conditions and Operating Parameters

ICP torch	Modified Sciex short torch: injector tube orifice diameter = 1 mm; 6-mm-o.d. x 4-mm-i.d. quartz tee attached at torch base
gas flow rates (L min^{-1})	
outer	16
auxiliary	1.3
make-up	0.26
nebulizer	0.4
forward power	1.4 kW
frequency	27 MHz
sampling position	18 mm from load coil, on center
sampler	Copper, 1.0-mm-diameter orifice
skimmer	Nickel, 0.9-mm-diameter orifice
detector voltage	-3900 V
ion lens setting	
bessel	-19.80 V
plate	-11.00 V
barrel	+5.42 V
photon stop	-7.46 V
operating pressures	
interface	1.5 torr
quadrupole chamber	3×10^{-5} torr

Table II. Chromatographic conditions

Separation of metalloproteins	
column	SynChrom, Inc. SynChroPak GPC 300 2-mm-i.d. x 250-mm-long
stationary phase	silica gel (5-μm particles, pore size = 300 Å)
mobile phase	0.1 M Tris/HCl (pH = 6.9)
eluent flow rate	100 μl min^{-1}
injection volume	3 μl
isotopes monitored	m/z = 78, 82, 42

Data Acquisition

The ICP-MS machine was equipped with the Elan 500 Upgraded hardware and software. During the separation of metalloproteins in serum two isotopes of selenium were measured (m/z 78 and 82), along with the calcium isotope at m/z 42. The data were acquired by peak hopping over the three isotopes using a 20 ms dwell time and 1 measurement per peak. Chromatograms were recorded in real time and stored on the hard disk of an IBM PS/2 Model 70 computer. These data were then processed as ASCII files in a spreadsheet program. The raw counts were smoothed using Golay smoothing. The peak area was determined by summing all the count rates under each peak. The background was measured while nebulizing only the mobile phase and summing the total counts under the particular chromatographic peaks.

Reagents and Samples

Deionized water (18 MΩ cm @ 25°C) obtained from a Barnstead Nanopure-II system (Newton, MA) was used. A 0.1 M tris(hydroxymethyl)aminomethane/ hydrochloric acid (tris/HCl) buffer was used as the mobile phase for the separation. Eluent of high ionic strength, such as 0.1 M NaCl, was not used to avoid plugging of the DIN. The Tris/HCl solution was prepared by dissolving certified ACS grade Tris (Fisher Scientific, Fair Lawn, NJ) in deionized water. The pH was then adjusted to 6.9 by adding concentrated Ultrex II grade HCl (J.T. Baker, Inc., Phillipsburg, NJ). Human serum (NIST SRM 909a-2) was reconstituted in 10 ml of the buffer solution.

RESULTS AND DISCUSSION

The determination of selenium compounds is complicated by the low ionization efficiency of selenium in the ICP, its presence in relatively low concentrations in real samples and the abundance of Ar related ions in the region of interest. During the separation of the metalloproteins in human serum, two molecular weight fractions were identified to contain selenium as shown in the chromatograms in Figures 2 and 3 (m/z 78 and 82 respectively). The first peak eluted at 4.6 minutes, followed by a second selenium containing peak at 6 minutes. Sodium elutes from the column at approximately 6.7 minutes and causes a decrease in the background at other masses and a negative peak in the chromatogram. Calcium was also identified at the same elution times as the selenium containing fractions shown in the chromatogram in Figure 4. A large calcium peak elutes later around 10.4 minutes. The size exclusion column was previously calibrated using pure protein standards (116). This calibration identifies the two selenium containing molecular weight fractions to be 200 and 15 kDa respectively.

Selenium exists as six isotopes including m/z 74 (0.9), 76 (9.0), 77 (7.6), 78 (23.5), 80 (49.8), and 82 (9.2). The natural percent abundance of each isotope is shown in parenthesis. Finding two isotopes of selenium free from mass spectral interference is difficult due to the argon related polyatomic ions in this mass region. Argon dimer ions exist at mass 76 ($^{40}Ar^{36}Ar$), 78 ($^{40}Ar^{38}Ar$), and 80 ($^{40}Ar_2$). ^{36}Ar is more abundant than ^{38}Ar and hence the background at mass 76 is larger than at 78. Due to the chloride in the matrix of human serum, $^{37}ArCl$ eliminates mass 77 as a possible selenium isotope. Other elements in the matrix such as Ca and K can also produce polyatomic interferences when combined with argon. Selenium at mass 74 gives a signal too weak to measure at the low concentration of selenium in human serum. After consideration of these

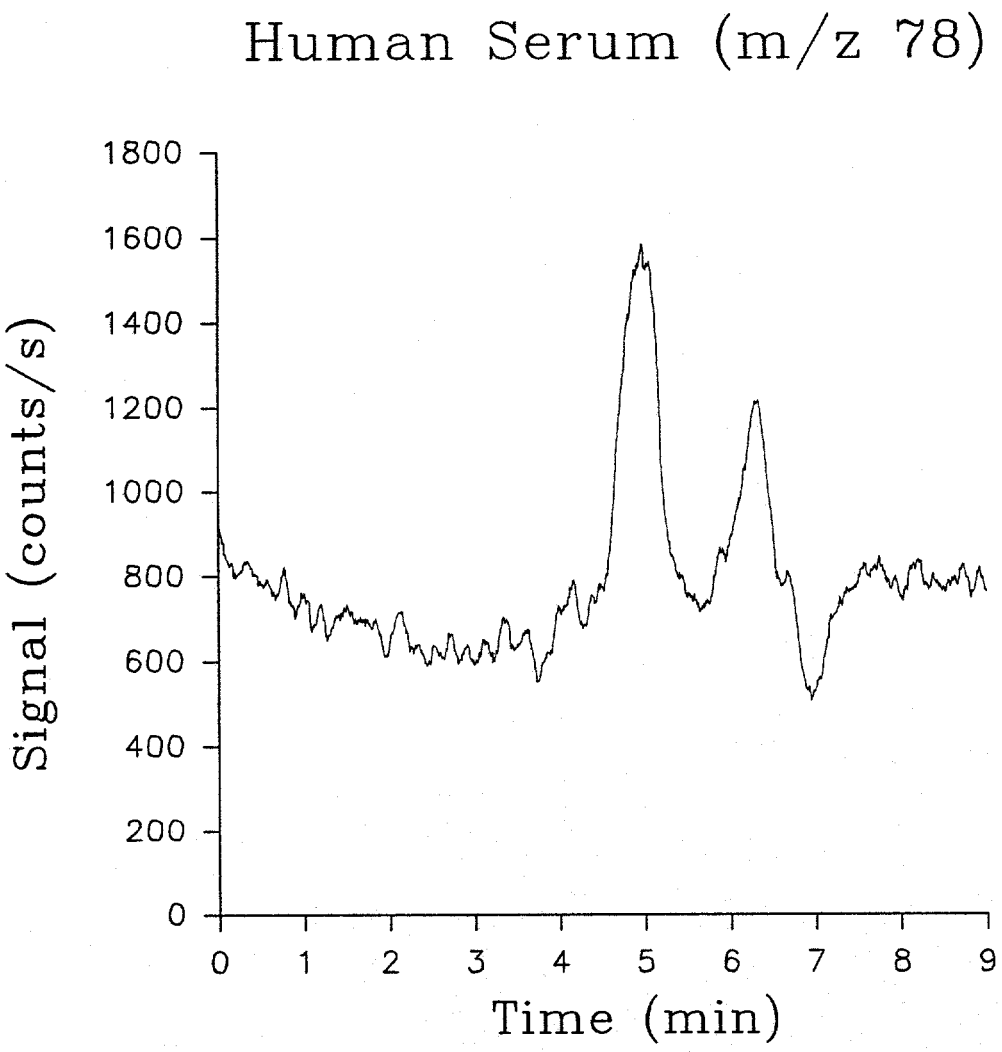

Figure 2. Selected ion chromatogram of metalloproteins in human serum monitoring m/z 78.

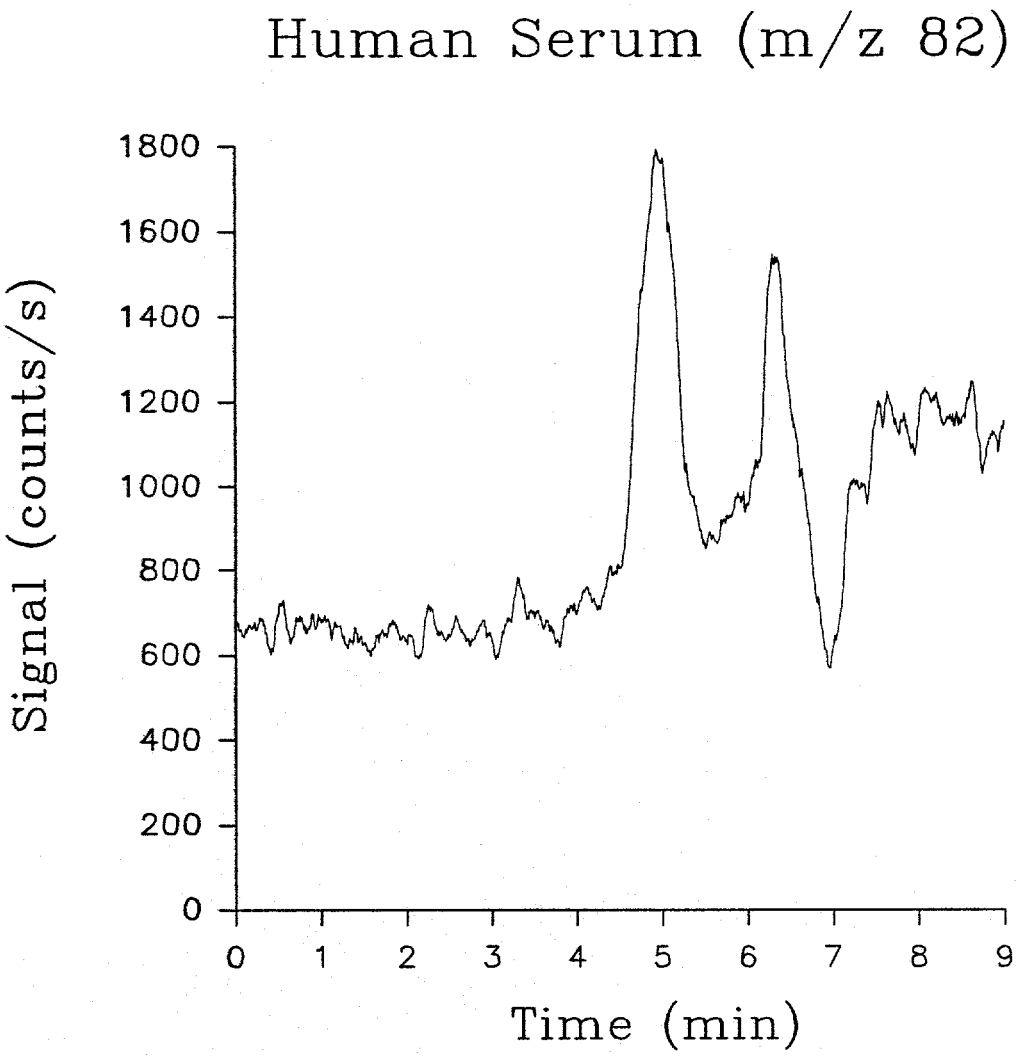

Figure 3. **Selected ion chromatogram of metalloproteins in human serum monitoring m/z 82.**

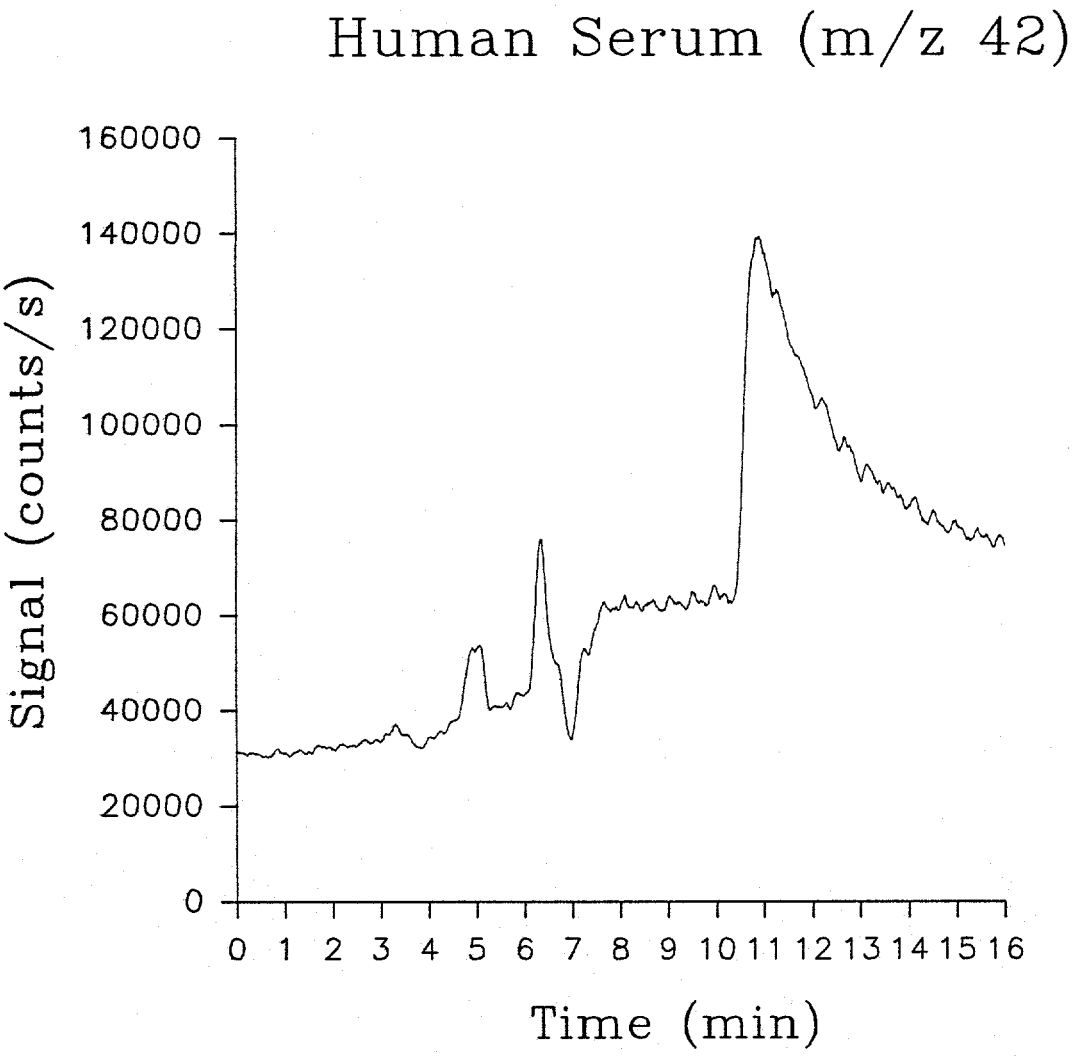

Figure 4. **Selected ion chromatogram of metalloproteins in human serum monitoring m/z 42.**

interferences, isotopes 78 and 82 were chosen to monitor selenium during the chromatographic separation. The correct isotope ratio of selenium 78 and 82 was not observed. An attempt was made to subtract the interference from $CaAr^+$ at m/z 82 by measuring another isotope of $CaAr^+$ at m/z 84. However, this data proved inconclusive due to species other than $CaAr^+$ at m/z 84. Hence, $CaAr^+$ does not seem to give a major contribution to m/z 84 or 82. Mass spectral interference from species in the human serum which coelute with the selenium containing molecular weight fractions cause background signal under the selenium peaks. The actual isotope ratio of selenium 78/82 is 2.55. The measured isotope ratio 78/82 (0.64 and 0.80 for peaks 1 and 2 respectively) is much lower than the actual isotope ratio, and therefore not only counts from selenium are present in the peaks at m/z 82. Because no other interference-free isotope of selenium exists, it is unclear if there is another ion at m/z 78 from an element that elutes at the same retention time as the selenium containing peaks. In order to accurately determine the amount of selenium in each peak, a second detection method which is free of mass spectral interference and has the capability to measure selenium at approximately 1.5 ppb is necessary.

The total selenium content in the serum was determined by the standard additions method to be 90 ppb. The plot of signal versus concentration of the added selenium spike has a R value of 0.9948 and is shown in Figure 5. An approximate concentration in each molecular weight fraction was determined by proportion at mass 78. By this method, the 200 kDa fraction contains 54 ppb and the 15 kDa fraction contains 36 ppb.

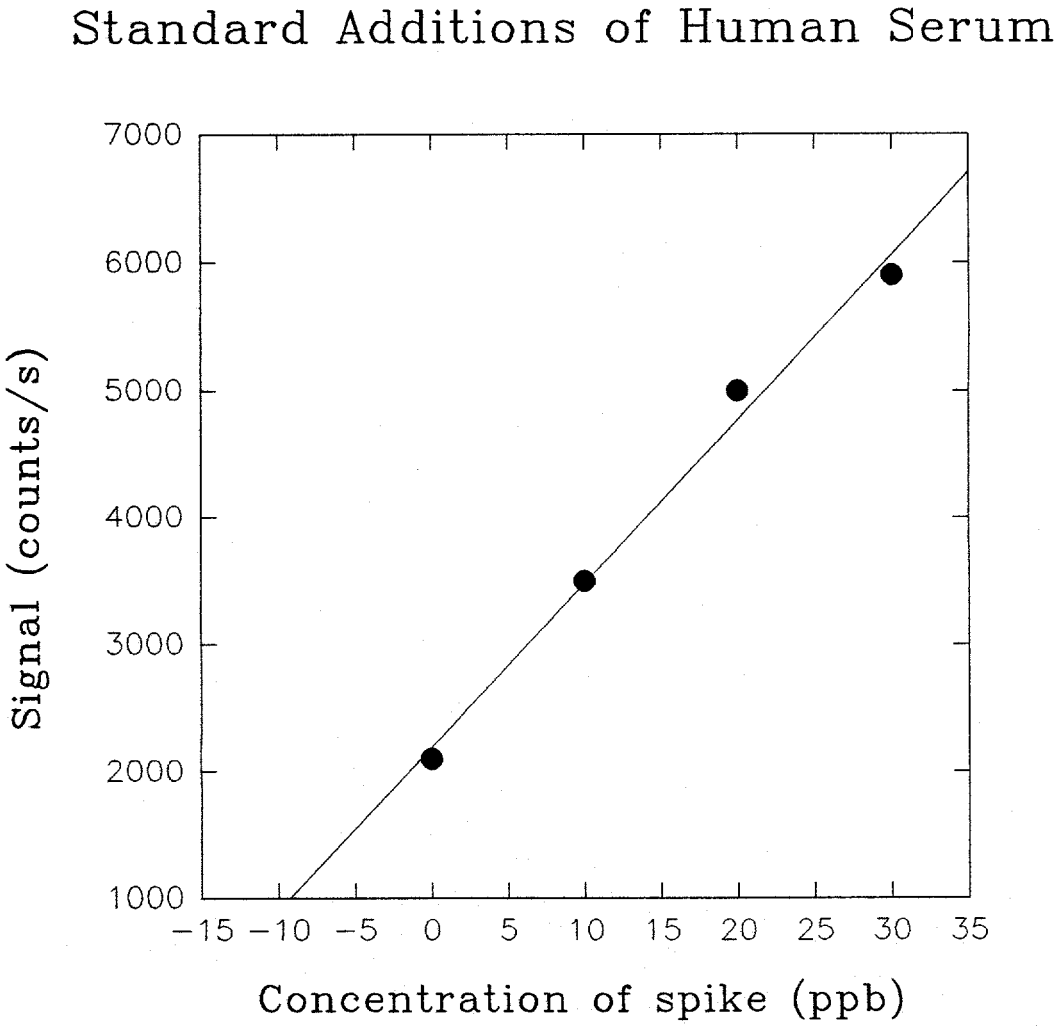

Figure 5. Standard additions plot for selenium in human serum (R = 0.9948).

CONCLUSION

Two molecular weight fractions in human serum containing selenium were observed. The total amount of selenium in human serum was determined by the standard additions method to be 90 ppb. Accurate determination of the amount of selenium in each fraction is hindered by mass spectral interferences due to species present in the serum sample which coelute with the selenium containing fractions.

PART II

THE EFFECTS OF XENON IN THE CENTRAL CHANNEL

OF THE INDUCTIVELY COUPLED PLASMA

INTRODUCTION

Mass spectrometry with the ICP offers relatively simple spectra in comparison to ICP atomic emission spectrometry. However, interference from polyatomic ions causes problems for certain elements. When aqueous samples are nebulized into an argon inductively coupled plasma (ICP), background species originate from argon, air, and water. For example, polyatomic ions are created from the combination of Ar, O, H, and N with each other and with other elements in the analyte matrix. Polyatomic ions including N_2^+, N_2H^+, NO^+, ArH^+, ClO^+, ArC^+, $ClOH^+$, ArN^+, and ArO^+ interfere in the measurement of atomic ion signals and isotope ratios for Si, K, V, Cr, and Fe. Previous work has shown that the addition of xenon in the central channel of the ICP attenuates these interferences (75).

Many spectroscopists have studied the ICP from a fundamental standpoint to better understand the relevant excitation/de-excitation and ionization/recombination processes responsible for the observed analyte atom and ion emission behavior. Fundamental properties such as electron number density and temperature including electron, excitation and ion temperatures have been extensively measured (118-140). The high temperature of the ICP is an important fundamental property in that it provides an excitation environment relatively free from dissociation and vaporization interferences and produces intense line spectra and therefore high analytical sensitivity. To further understand the influence of xenon on excitation and ionization in the plasma, and the reasons for the reduction of polyatomic ions, the excitation temperature (T_{exc}) of the ICP was measured with various amounts of xenon added to the central channel.

Theory

The excitation temperature is a measure of the population density of electronically excited states and can be experimentally determined from a Boltzmann plot. For a system in local thermal equilibrium (LTE), the population density of an atomic or ionic level p follows a Boltzmann distribution (141-142) as described by the following equation,

$$n(p) = n[g_p/Z(T)]\exp(-E_p/kT) \qquad (1)$$

where n(p) is the population density of atoms or ions in level p, n is the total concentration of neutral atoms or ions, g_p is the statistical weight of level p, Z(T) is the partition function, E_p is the excitation energy for level p, k is the Boltzmann constant (8.62×10^{-5} eV/K), and T is the excitation temperature. The intensity of emission observed (I_{pq}) when an excited state p emits to a lower state q is as follows,

$$I_{pq}\ (\text{ergs/srs}\cdot\text{cm}^2) = [(l/4\pi)n(p)A_{pq}hc]/\lambda_{pq} \quad (2)$$

where l is the pathlength of the source, A_{pq} is the transition probability for spontaneous emission, h is Planck's constant, c is the speed of light, and λ_{pq} is the wavelength of the emission observed. By the combination of equations (1) and (2) the following equation can be derived and used to create a Boltzmann plot (143),

$$\ln(I_{pq}\lambda_{pq}/g_pA_{pq}) = -E_p/kT_{exc} + \ln[nlhc/4\pi Z(T)] \quad (3)$$

where E_p is the excitation energy in eV. T_{exc} can be calculated from the slope (-1/kT) of a plot of $\ln(I_{pq}\lambda_{pq}/g_pA_{pq})$ versus E_p.

In localized regions, the ionization of metal atoms can be considered as an equilibrium process in many flames and plasmas ($M \Leftrightarrow M^+ + e^-$). This ionization is described by the Saha equation for the ionization constant K_i,

$$K_i = n_{M+}n_e/n_M$$

where n_e is the number density of free electrons.

The Saha equation is as follows,

$$\log K_i = 15.684 + \log Z_{M+}/Z_M + 3/2\log T - 5040E_{ion}/T$$

where Z_i's are partition functions for the ion and the neutral atom and E_{ion} is the ionization energy in eV. Small values of E_{ion} and high temperatures favor the formation of ions. Also, a decrease in temperature will have a greater effect on the degree of ionization of species having a high ionization energy. Oxygen, nitrogen, hydrogen, and argon all have high ionization energies of 13.6, 14.1, 13.598 and 15.76 eV respectively. It is proposed that if xenon cools the plasma this decrease in temperature will have greater effect on the polyatomic ions than on the analyte ions, as experimentally observed (144).

EXPERIMENTAL SECTION

Instrumentation

A schematic diagram of the instrumental setup is shown in Figure 1. The ICP torch was mounted in the Perkin-Elmer Sciex ELAN Model 250 ICP Mass Spectrometer. The center section of the shielding box surrounding the ICP-MS interface was removed to allow optical emission measurements from the ICP. A 100 ppm Fe solution was prepared from a 1000 μg/ml PlasmaChem Associates (Bradley Beach, NJ) standard. Deionized water (18 MΩ cm @ 25°C) obtained from a Barnstead Nanopure-II system (Newton, MA) was used for dilution. The solution was introduced by a peristaltic pump and nebulized by a CETAC ultrasonic nebulizer (Model U-5000). The xenon (Spectra Gases, Newark, NJ) was specified to be 99.9% pure and was introduced into the nebulizer flow through a quartz tee (5 mm i.d.) at the base of the torch to alleviate contamination of the sample introduction system with xenon. The ICP operating parameters were optimized to give the greatest sensitivity for Fe (I) and Fe (II) emission. A slightly lower aerosol gas flow rate than the optimum for ICP-MS was necessary in order to see the Fe ion emission. A gas flow rate of 1.12 LPM was chosen instead of the usual 1.40 LPM. A higher aerosol gas flow rate pushes the ionization zone closer to the sampler, which is better for ICP-MS. Unfortunately, the ions are then extracted into the vacuum system before they can be excited and produce emission.

The emission of various Fe (I) and Fe (II) lines in the ICP was focused by a lens onto the entrance slit of a monochromator described in Table I. A photomultiplier tube was used to detect the signals which were measured by a Keithley 485 autoranging picoammeter and then recorded on a Houston Instrument Omnigraphic 2000 x-y

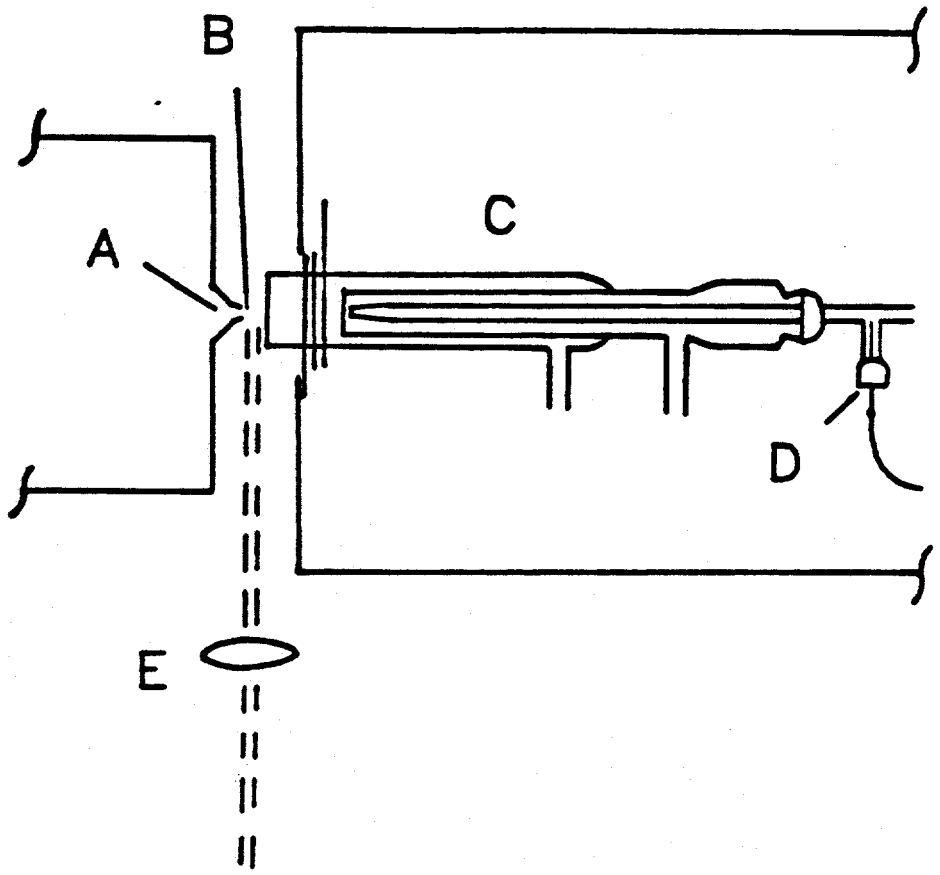

Figure 1. Instrumental setup for observation of Fe (I) and Fe (II) emission from the ICP. A = sampler on ICP-MS interface, B = region viewed by monochromator, C = ICP torch, D = quartz tee for the introduction of xenon, E = lens. Reproduced from reference (144) with permission.

Table I. Instrument Conditions and Operating Parameters

ICP torch	Ames Laboratory design (27), outer tube extended 30 mm from inner tube
gas flow rates (L min^{-1})	
outer Ar	15
auxiliary Ar	0
nebulizer gas	
Ar (L min^{-1})	1.12
Xe (mL min^{-1})	0, 2.24, 8.96, 16.8
forward power	1.25 kW
frequency	27 MHz
Ultrasonic nebulizer	CETAC Technologies (Omaha, NE) Model U-5000 current setting 6 (arbitrary units) desolvation heater temperature 140°C desolvation condenser temperature 0°C
Monochromator	Jarrell-Ash Division
Ebert mount	Model 82000 focal length 0.5 m grating 1160 grooves/mm blazed at 250 nm
Photomultiplier	Thorn EM Model R955 bias voltage
Mass Flow Controller	Matheson Model 8200

recorder. The instrument conditions and operating parameters chosen are summarized in Table I.

Fe (I) and Fe (II) levels

Several criteria must be used when selecting the lines to successfully create a Boltzmann plot (143). These criteria include: (1) the wavelengths are close together to avoid the calibration of the detector system, (2) the lines must have reliable A_{pq} values, (3) they must span a wide range in excitation energy to enhance precision, and (4) their intensities should provide reasonable signal to noise ratios. The Fe (I) and Fe (II) lines chosen for this study are displayed with their ionization energies and gA values in Tables II and III respectively. Abel inversion is a technique used in optical experiments to construct radial emission profiles from line-of-sight intensity measurements (145). In this experiment, emission was only observed from the gas flowing into the sampler. Due to the radially resolved nature of ICP-MS, Abel inversion was unnecessary.

Table II. Wavelengths, excitation energies, and gA values for Fe (I) lines measured to create Boltzmann plots.

λ (nm)	E (eV)	gA (x 10^8 s^{-1}) (146)
381.58	4.73	8.15
376.55	6.53	15.9
374.95	4.22	7.02
373.71	3.37	1.29
373.49	4.18	9.76
371.99	3.33	1.79
361.88	4.42	5.09
360.89	4.45	4.16
360.67	6.13	11.7
360.55	6.17	6.31
357.01	4.39	7.56
356.54	4.44	7.99

Table III. Wavelengths, excitation energies, and gA values for Fe (II) lines measured to create Boltzmann plots.

λ (nm)	E (eV)	gA ($X10^8$ s^{-1})	ref. no.
275.57	5.48	21.1	147
275.33	7.77	24.8	147
274.65	5.59	11.7	148
274.32	5.62	7.20	148
273.95	5.61	15.4	148
273.07	5.62	1.00	148
271.44	5.55	3.86	147
266.66	8.07	24.1	147
266.47	8.04	26.5	147
262.83	4.84	3.43	148
262.57	4.77	3.35	148
262.17	4.85	0.97	148
261.76	4.82	2.62	148
261.38	4.85	3.98	148
261.19	4.79	8.71	148
260.71	4.84	6.63	148
259.94	4.77	22.1	148
259.84	4.82	7.85	148
258.59	4.79	6.44	148
258.26	5.88	3.09	148
256.69	5.91	2.60	147
256.35	5.88	5.21	148
256.25	5.82	12.8	147

RESULTS AND DISCUSSION

Excitation Temperature

To create a Boltzmann plot of $\ln(I_{pq}\lambda_{pq}/g_pA_{pq})$ versus E_p, the relative intensities of several emission lines of a range of ionization energies must be measured. The Fe (I) emission lines measured in this study are shown in Table II with their corresponding excitation energies and gA values. Emission from Fe (I) lines was observed with 0, 0.2, 0.8, and 1.5% xenon added to the central Ar flow. These percentages correspond to 0, 2.24, 8.96, and 16.8 ml/min respectively. Boltzmann plots were created for each amount of xenon added (Figures 2-5). For comparison, Boltzmann plots for 0 and 1.5% xenon for Fe (I) are shown on the same graph in Figure 6. As can be seen in the figure, xenon had essentially no effect on the slope of the plot for Fe (I) and therefore no effect on the T_{exc}. Also, xenon had little effect on the intensities of the lines as shown by the similarity in the points on the two plots of 0 and 1.5% xenon added. The calculated excitation temperatures for each amount of xenon added are given in Table IV along with the standard deviation in each temperature value. The average T_{exc} was found to be 6658 K.

Emission from Fe (II) lines was also observed with 0, 0.2, 0.8, and 1.5% xenon added to the central channel. Boltzmann plots were created for each addition and are shown in Figures 7-10. The addition of xenon caused a modest increase in the slope of the Fe (II) Boltzmann plot as seen when the data for 0 and 1.5% xenon added are shown on the same graph (Figure 11). The increase in slope corresponds to a decrease in T_{exc} as shown in Table V. T_{exc} with no xenon added was calculated to be 8121 K whereas with 1.5% xenon added, the temperature decreased to 7094 K. The degree of ionization (α_{M+}) can be calculated as follows,

$$\alpha_{M+} = (K_{ion}/n_e)/(1 + K_{ion}/n_e)$$

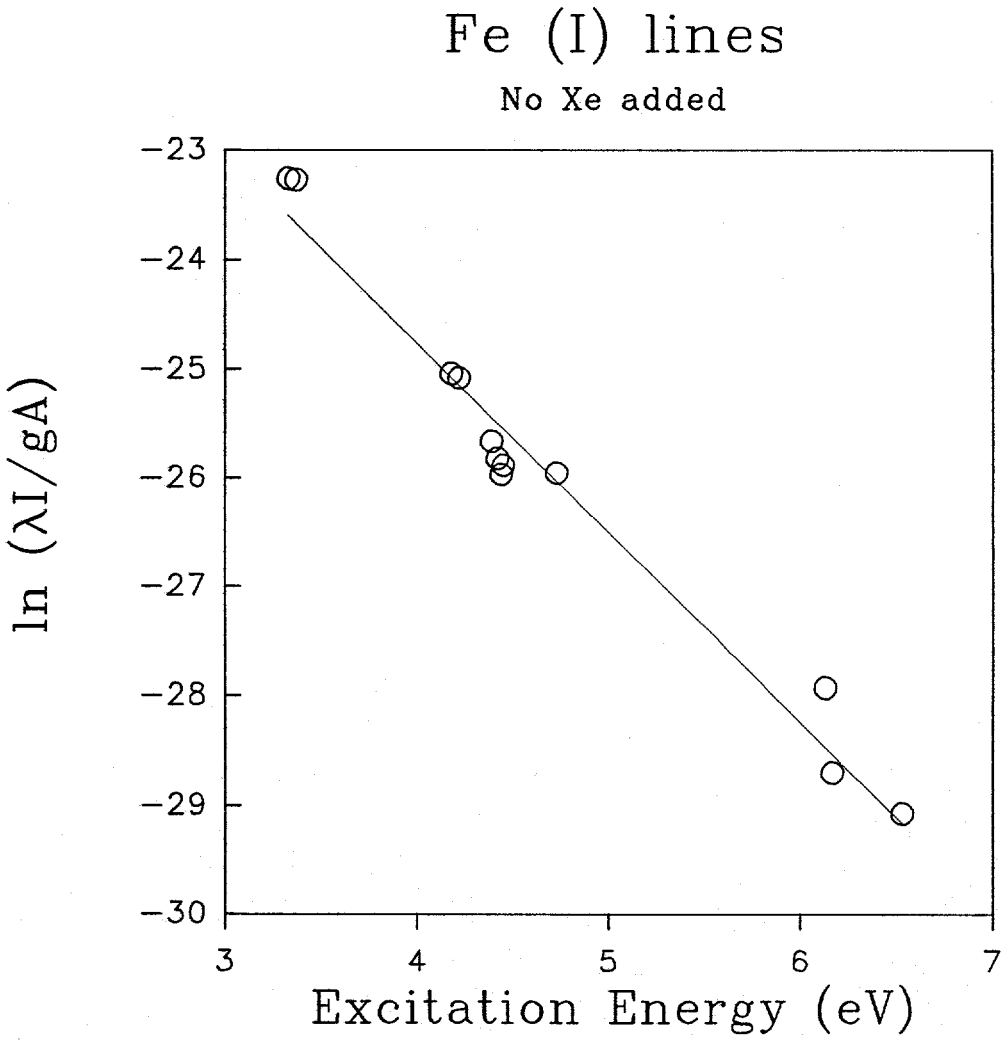

Figure 2. Boltzmann plot for emission from Fe (I) lines with no xenon added to the central channel of the ICP.

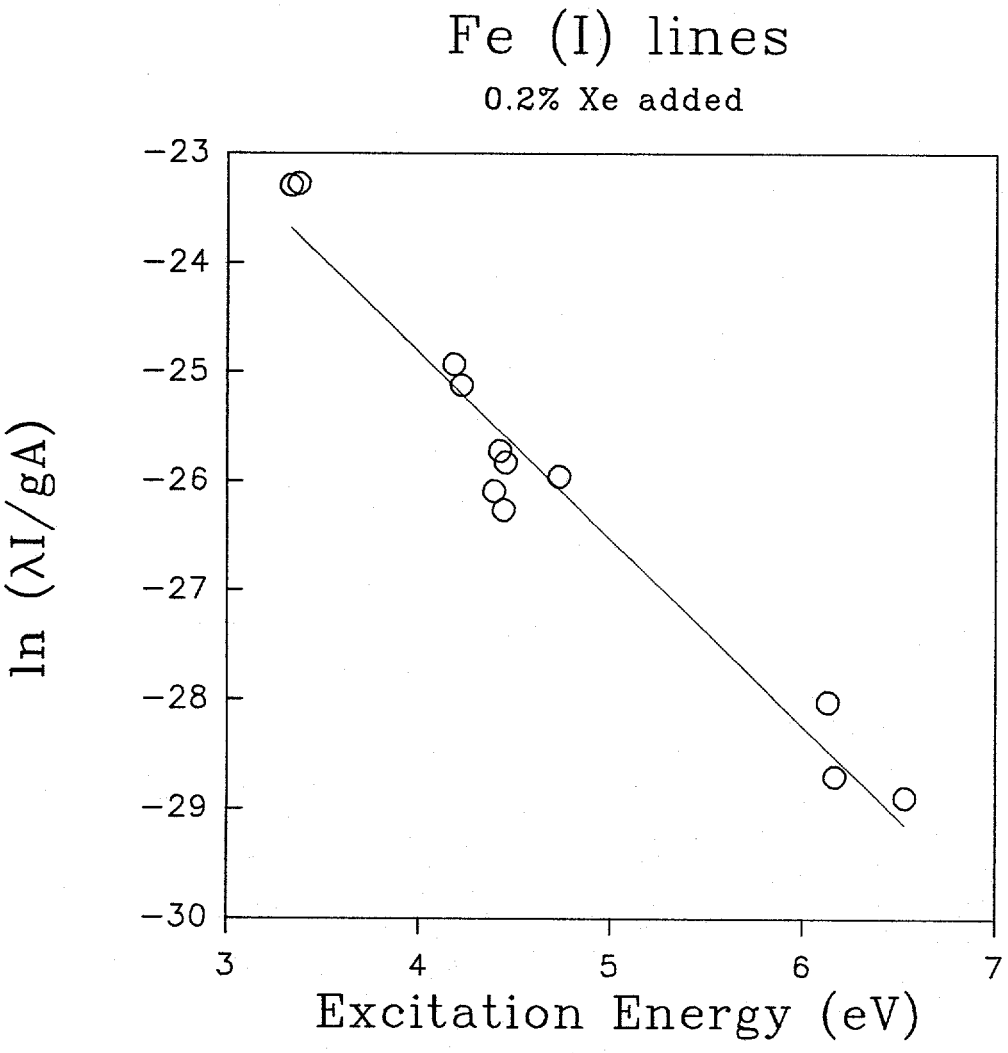

Figure 3. Boltzmann plot for the emission of Fe (I) lines with 0.2% xenon added to the central channel of the ICP.

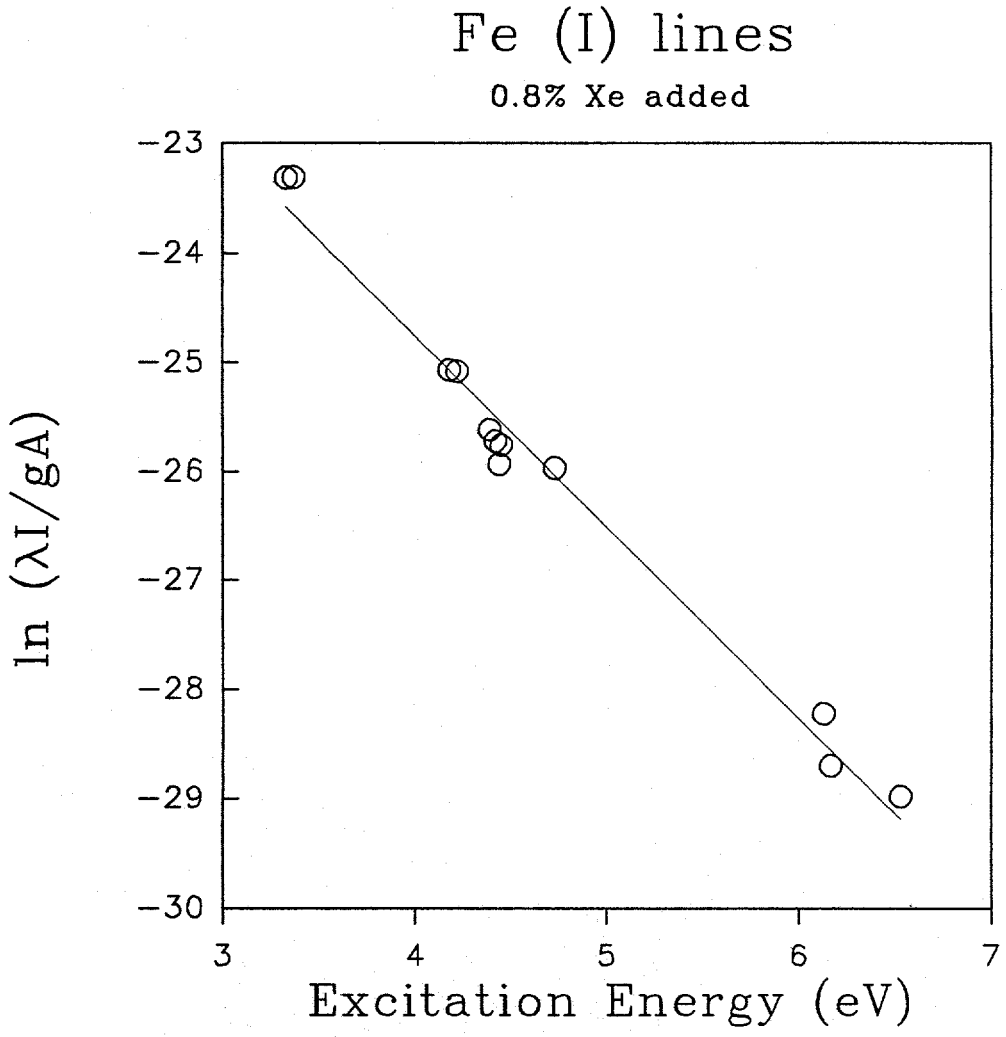

Figure 4. Boltzmann plot for the emission of Fe (I) lines with 0.8% xenon added to the central channel of the ICP.

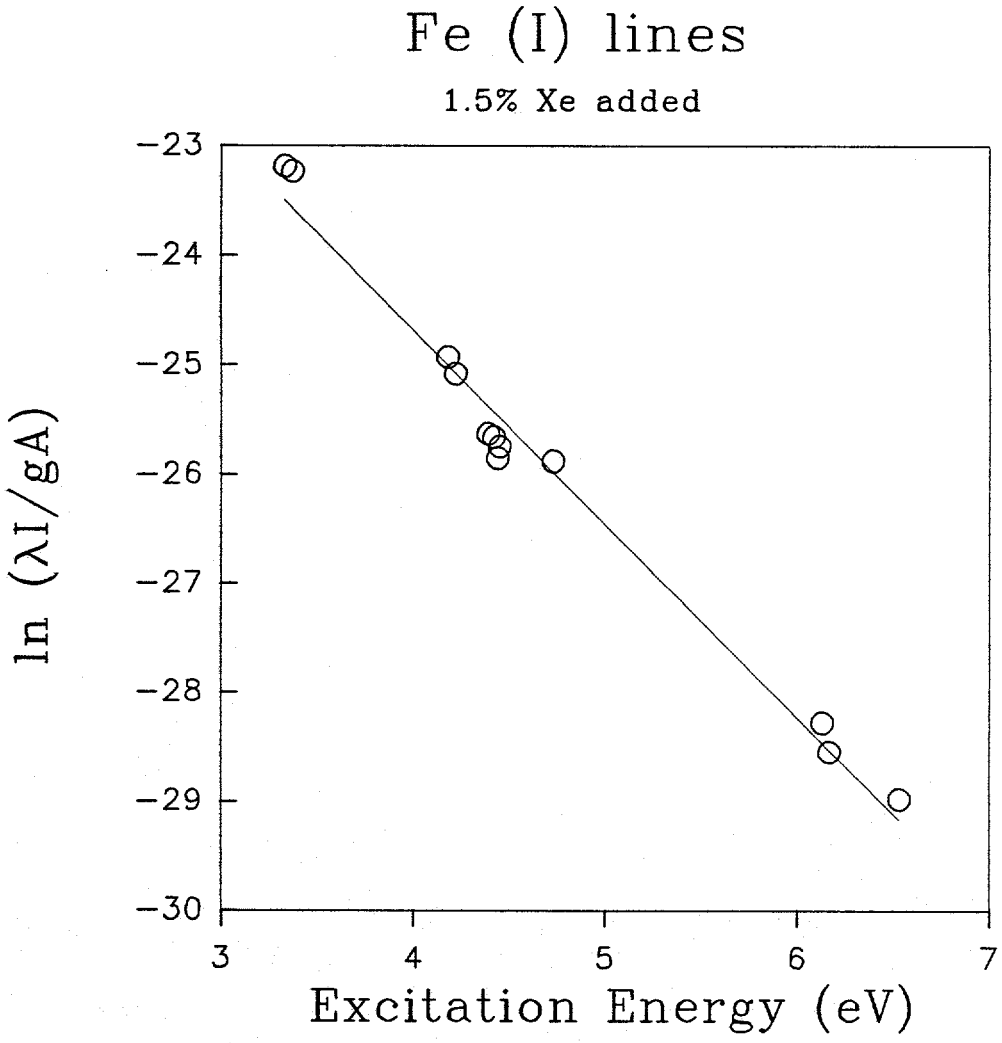

Figure 5. Boltzmann plot of emission from Fe (I) lines with 1.5% xenon added to the central channel of the ICP.

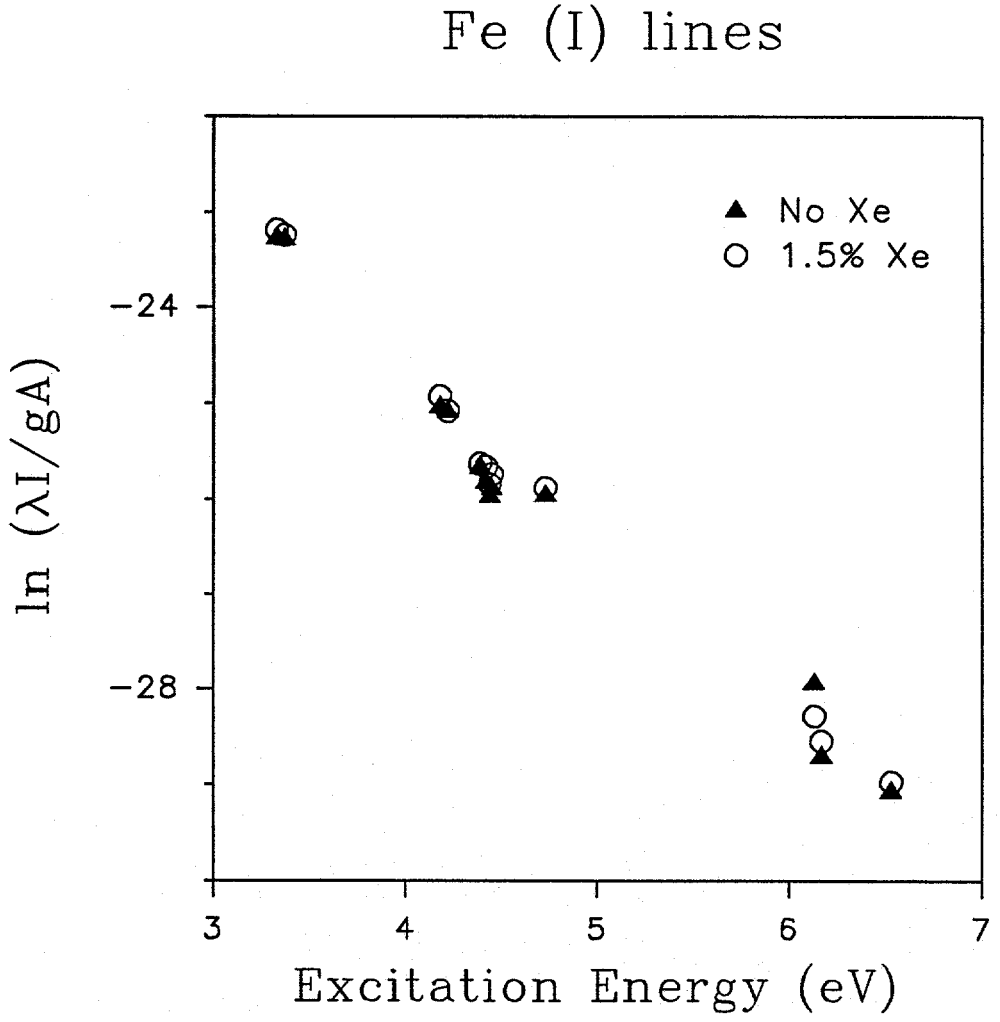

Figure 6. Boltzmann plots for the emission of Fe (I) lines with 0 and 1.5% xenon added to the central channel of the ICP.

Table IV. T_{exc} values from measurements of Fe (I) emission with the addition of Xe. Standard deviation values, calculated from the standard deviations of the slopes, are given in parentheses.

%Xe[a]	T_{exc} (K)
0.0	6675 (362)
0.2	6797 (466)
0.8	6617 (273)
1.5	6544 (275)

[a] Percent of nebulizer flow.

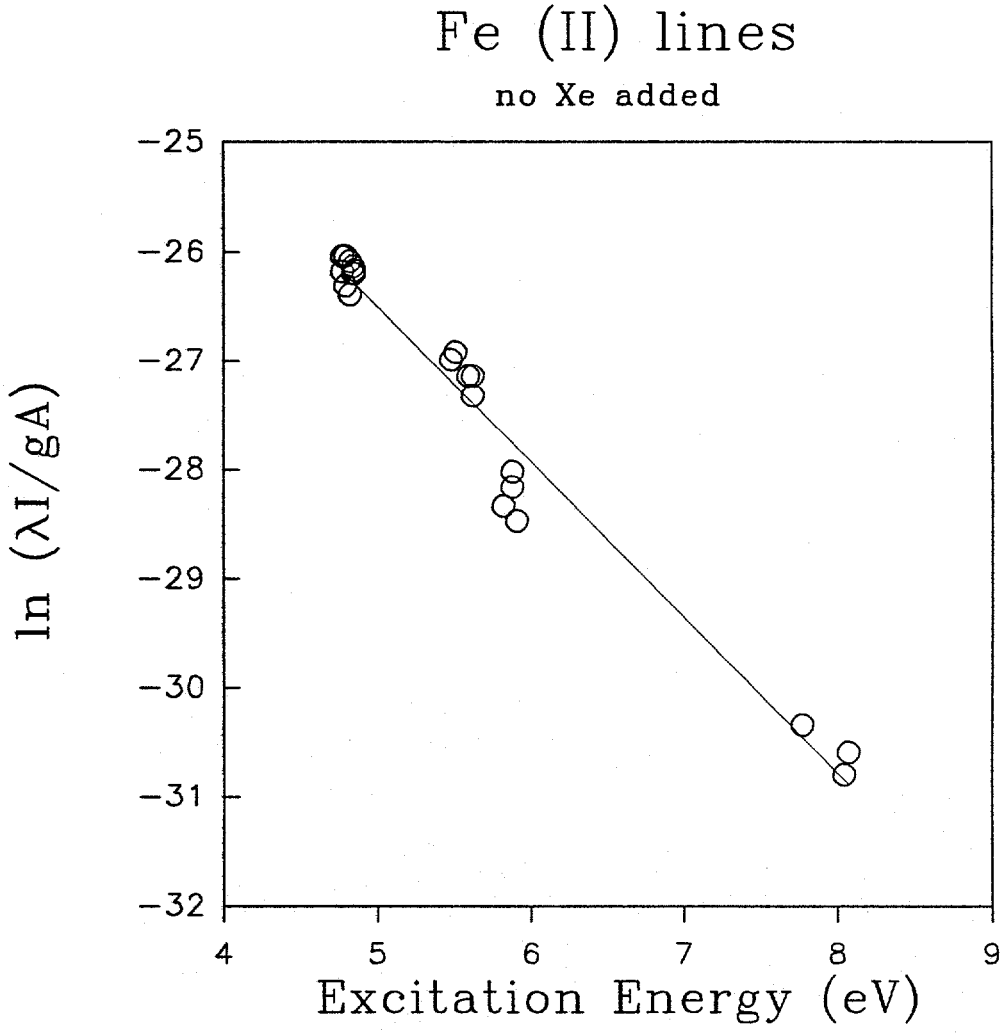

Figure 7. Boltzmann plot for the emission of Fe (II) lines with no xenon added to the central channel of the ICP.

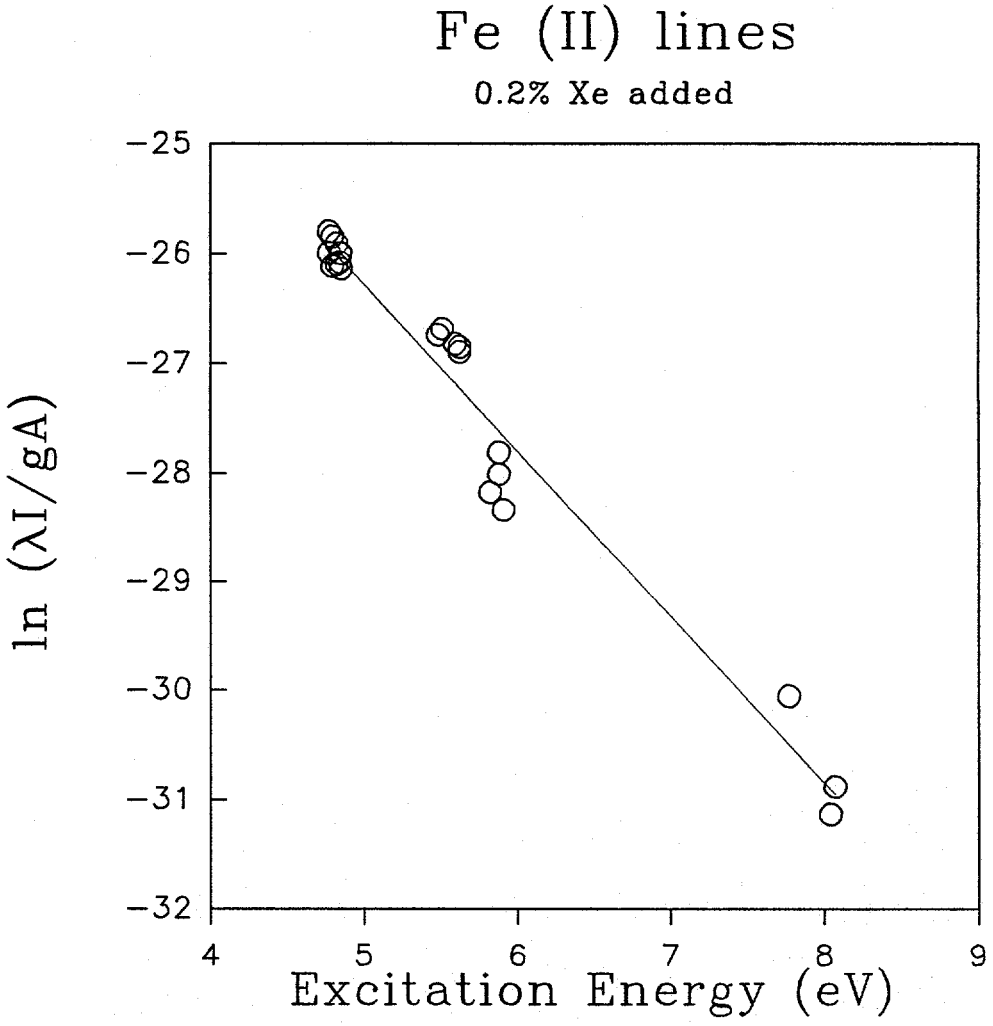

Figure 8. Boltzmann plot for the emission of Fe (II) lines with 0.2% xenon added to the central channel of the ICP.

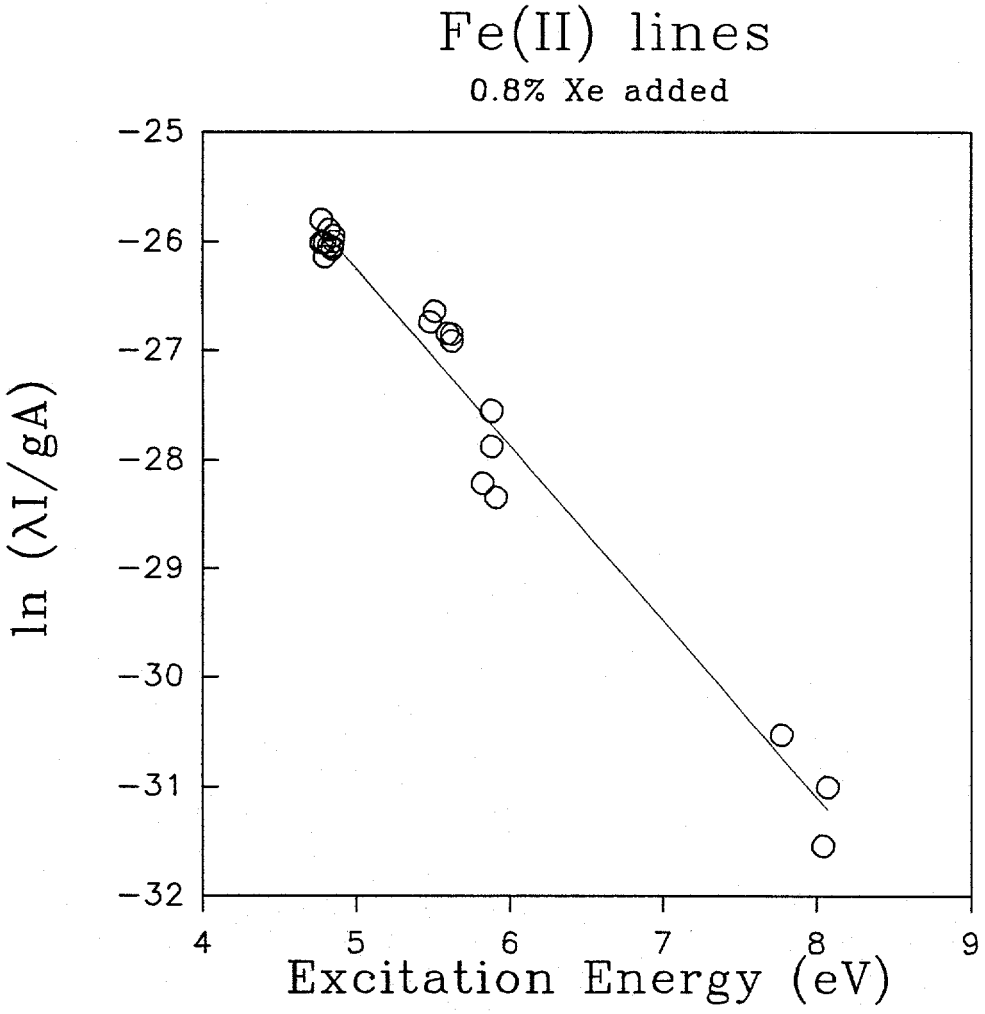

Figure 9. Boltzmann plot for the emission of Fe (II) lines with 0.8% xenon added to the central channel of the ICP.

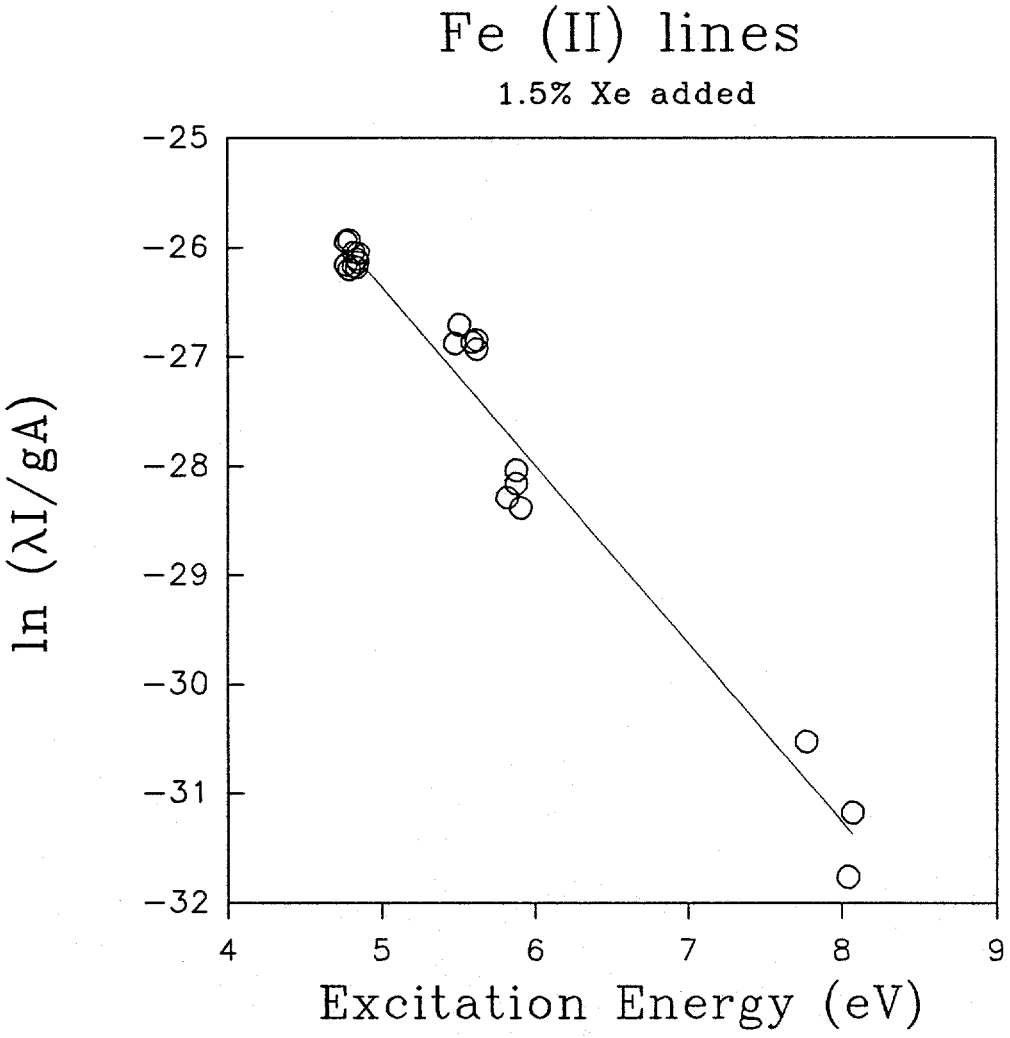

Figure 10. Boltzmann plot for the emission of Fe (II) lines with 1.5% xenon added to the central channel of the ICP.

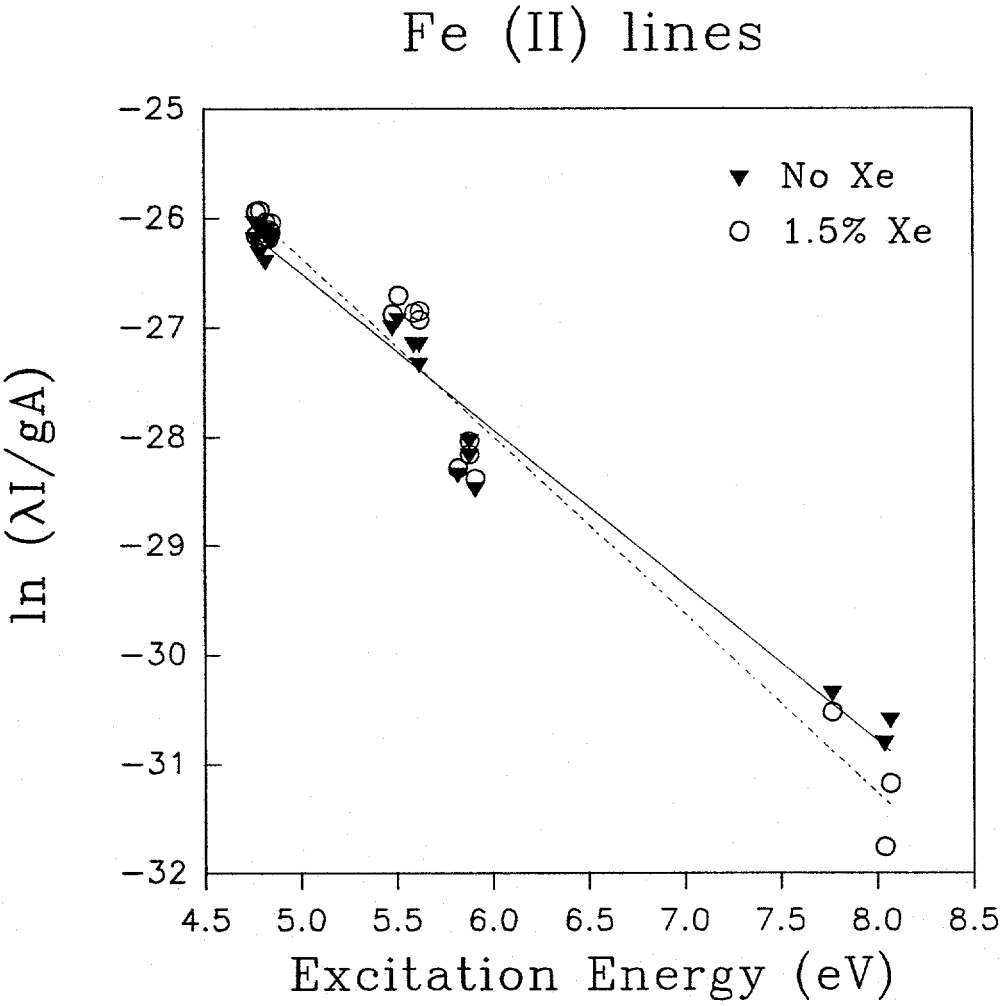

Figure 11. Boltzmann plots for the emission of Fe (II) lines with 0 and 1.5% xenon added to the central channel of the ICP.

Table V. T_{exc} values from measurements of Fe (II) emission with the addition of Xe. Standard deviation values, calculated from the standard deviation in the slopes, are given in parentheses.

%Xe[a]	T_{exc} (K)
0.0	8121 (425)
0.2	7617 (398)
0.8	7168 (348)
1.5	7094 (381)

[a]Percent of nebulizer flow.

where n_e is the electron number density and K_{ion} is calculated from the Saha equation. In order to calculate K_{ion}, the partition functions can be calculated for a particular temperature using polynomial coefficients tabulated in the literature (149), and the following equation,

$$Z(T) = A(T/10^3)^2 + B(T/10^3) + C,$$

where A, B, and C are the tabulated coefficients and T is the temperature. By this method, the degree of ionization of Fe at 8121 K is calculated to be 98.40%, using a n_e of 1×10^{15} cm^{-3} as determined previously (144). The calculation at a temperature of 7094 K gives a degree of ionization of 91.13%. Therefore, with the temperature decrease due to the added xenon a calculated decrease in the number of ions is 7.3%. Experimentally, the Fe^+ signal with 10 ml/min xenon added was only 6% of that without Xe, a 94% loss of ions (144). A temperature decrease from 8121 K to 7094 K lowers the degree of ionization of oxygen to a greater extent than that of iron due to the higher ionization energy of oxygen. Calculations give the degree of ionization of oxygen to decrease 20 times (from 0.5653% to 0.02759%) with this temperature decrease. Therefore, polyatomic ion levels will decrease by a greater extent than analyte ions of lower ionization energies. For example, the signals from ArO^+ (m/z 56) and ArN^+ (m/z 54) were experimentally observed to decrease by 99.1% and 98.3% respectively when xenon was added at 10 ml/min (144). Due to a greater experimental decrease in ions than that calculated for the temperature decrease found due to added xenon, another mechanism is involved in the alleviation of polyatomic ions. One proposed process is that Xe^+ causes a matrix effect similar to the addition of Cs^+. More experimental work is necessary to determine its validity.

The value for T_{exc} found in this study with no Xe added by measuring Fe (II) lines is in good agreement with Walker and Blades value of 8180 K (143). Walker and Blades'

measurement was taken in a 1.25 kW plasma with an aerosol gas flow rate of 0.9 LPM. Experimental conditions greatly influence plasma parameters (125, 128-130, 150). For example, Robin and associates found that temperature and electron number density decrease with increasing generator frequency (137). Increasing the RF power causes an increase in the excitation temperature (124, 132). However, increasing the aerosol gas flow rate causes a decrease in the excitation temperature (130, 132). Even when these factors are taken into account, literature values for T_{exc} widely differ (3000 to 7000 K). These discrepancies are only partly a result of the uncertainty in A values (151).

Charge Transfer

The emission studies also showed that xenon affects the population of various Fe (II) excited states differently. It follows that different processes are involved in the population of these levels. One possible process for the population of a particular level is a charge transfer reaction. In this study, the proposed charge transfer reaction takes place between an excited state of the xenon ion and the iron neutral. Plots of normalized intensity versus %Xe added for five different emission lines are shown in Figure 12. The percent increase in signal with added xenon is greatest for lines from states at 5.48 and 5.59 eV. Less increase was found for the 4.77 and 5.82 eV states, and a substantial decrease in signal was found for the 8.07 eV state. An energy level diagram showing the pertinent states of Xe and Fe is shown in Figure 13 (152). The ionization energy of xenon is 12.127 eV and an excited state ($^2P_{1/2}$) of the ion exists at 13.44 eV. This excited state is resonant with the excited states of the Fe^+ at 5.59 and 5.48 eV, corresponding to wavelengths of 274.65 and 275.57 nm. This resonance is clear in an expanded diagram showing only the energy levels above 12 eV (Figure 14). The greater enhancement of these lines over lines above and below this energy state is possible evidence for the

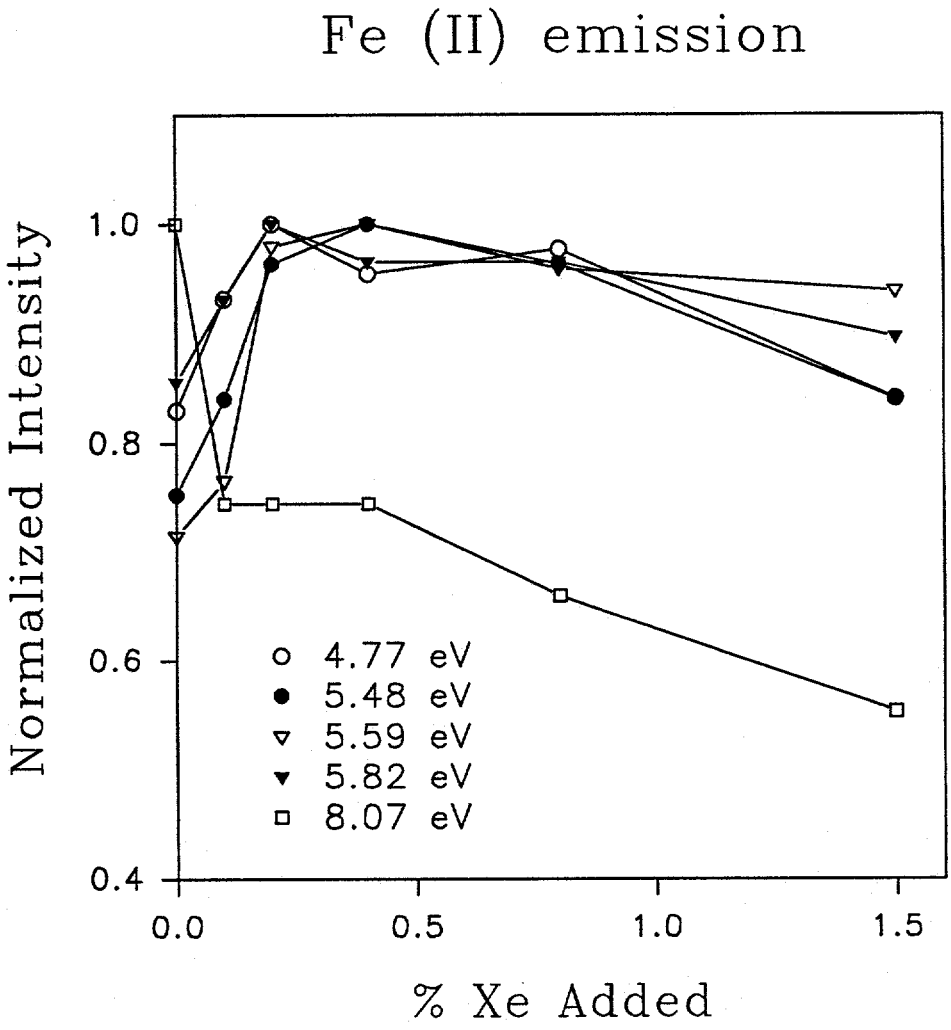

Figure 12. Plot of normalized emission intensity versus percent xenon added to the central channel of the ICP for several Fe (II) lines of various excitation energies.

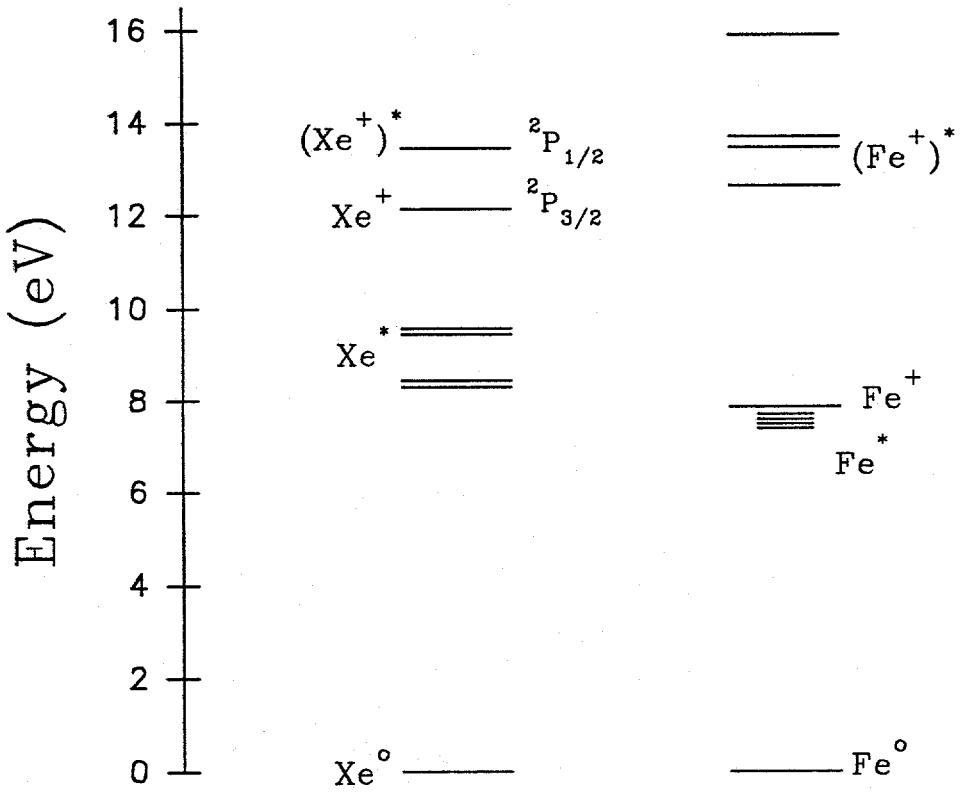

Figure 13. Energy level diagram showing some of the states of xenon and iron below 16 eV.

following charge transfer reaction:

$$Fe^0 + (Xe^+)^* \rightarrow (Fe^+)^* + Xe^0 + dE$$

Other investigators have studied the role of charge transfer as an ionization and excitation mechanism. Robin suggested that charge transfer reactions take place in the ICP when the total excitation energy (the sum of the ionization and excitation energy) of a particular level equals approximately the ionization potential of argon (15.8 eV) (153). Charge transfer processes in the ICP involving Ar^+ and metal atoms including Cu and Mn have been previously studied by Goldwasser and Mermet (154). By measuring line intensity ratios they found that states of Cu above the ionization limit of Ar and states resonant with Ar^+ are not excited by the same processes. The emission originating from the line resonant with the 16 eV limit was found to be stronger than lines from nearby states. Farnsworth found that charge exchange between ground state magnesium atoms and ground state argon ions is the primary mechanism by which the Mg II $4s^2S$ and $3d^2D$ levels are populated (155). Farnsworth also concluded that as long as momentum is conserved, the energy defect can be supplied in the form of kinetic energy of colliding partners and therefore levels with total excitation energies within kT of 15.94 eV (the ionization limit of Ar) should be considered as candidates for population by charge exchange (155).

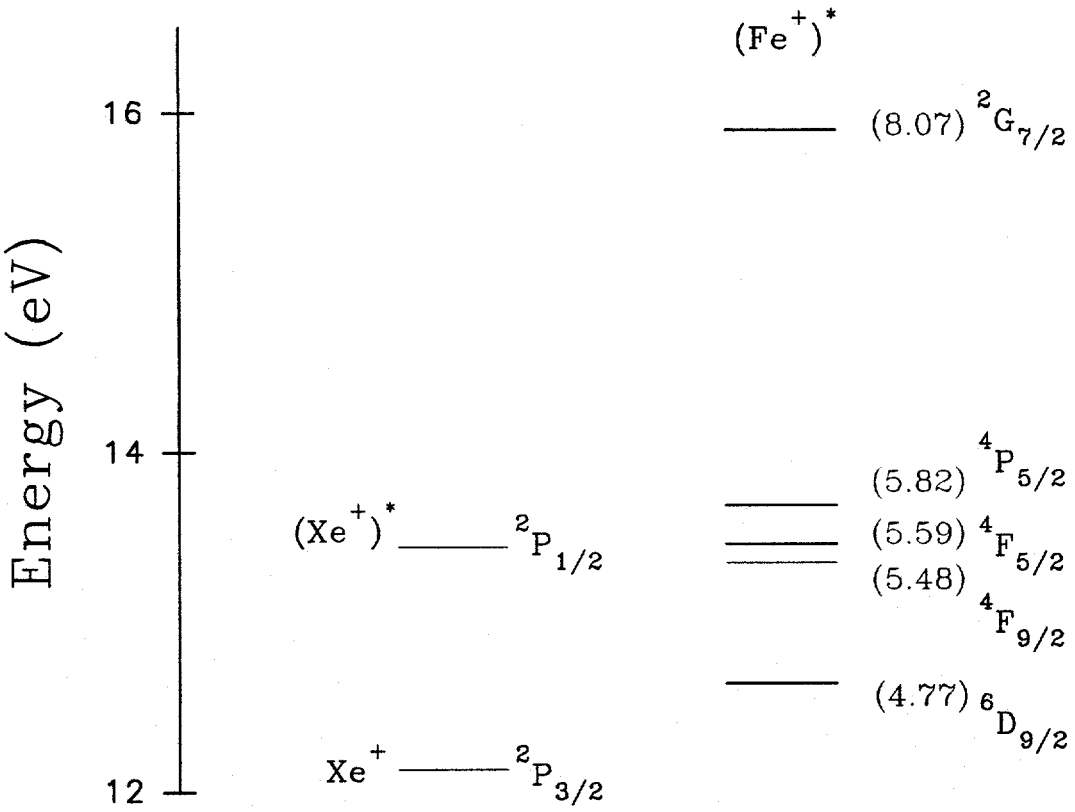

Figure 14. Energy level diagram showing states of xenon and iron between 12 and 16 eV.

CONCLUSION

Fundamental properties of the ICP are measured to understand the mechanisms responsible for the observed atom and ion behavior. The excitation temperature of the ICP was determined to understand the observed decrease in ion abundance in ICP-MS with the additon of xenon to the central channel. T_{exc} calculated by the measurement of Fe (II) lines was found to only slightly decrease with the addition of xenon into the central channel. No change in temperature was found by measurement of Fe (I) lines. The temperature decrease found with the Fe (II) lines does not account for the loss of iron ions previously measured with the addition of xenon. Therefore, a decrease in temperature of the ICP is not solely responsible for the observed loss of analyte and polyatomic ions in ICP-MS with the addition of xenon. It is possible that xenon behaves as a matrix ion. However, more experimental work is necessary to determine the validity of this proposal.

A charge transfer reaction is a proposed process of populating the Fe^+ excited states resonant with the $^2P_{1/2}$ state of xenon. These states were found to have enhanced emission intensity over the states above and below the $^2P_{1/2}$ state. Charge transfer reactions have been previously known to occur between metal atoms and argon ions in the ICP. It is therefore possible that these reactions could take place between metal atoms and xenon ions. This study represents the first evidence for such reactions involving ions other than Ar^+ in the ICP.

GENERAL CONCLUSIONS

ICP-MS has been used in a wide variety of applications. One such application is the speciation of elements by chromatography while employing ICP-MS for element specific detection. These experiments combine the high analytical sensitivity of ICP-MS with the power of separation of chromatography, allowing trace elemental speciation of elements important in environmental, biological, and human health applications. ICP-MS is a well established analytical technique. However, efforts are still made to increase its utility by further optimization of the technique, such as lowering of detection limits, and decreasing interferences from polyatomic ions.

The primary goals of this work included the speciation of selenium in Part I and an effort to understand xenon's role in the alleviation of polyatomic ions in ICP-MS in Part II. Size exclusion chromatography successfully separated two molecular weight fractions in human serum containing selenium. ICP-MS was able to detect as low as 1.5 ppb selenium contained in the lowest weight fraction after dilution in the buffer as the fraction elutes through the column. In Part II, a decrease in T_{exc} due to the added xenon was concluded not to be solely responsible for the decrease in analyte and polyatomic ions in ICP-MS. Also, evidence for a possible charge transfer reaction between an excited state of xenon ion and the neutral iron was presented.

LITERATURE CITED

1. Houk, R. S.; Fassel, V. A.; Flesch, G. D.; Svec, H. J.; Gray, A. L.; Taylor, C. E. *Anal. Chem.* **1980**, *52*, 2283.

2. Jarvis, K. E.; Gray, A. L.; Houk, R. S. *Handbook of Inductively Coupled Plasma Mass Spectrometry*; Blackie: Glasgow, **1991**.

3. Doherty, W. *Spectrochim. Acta* **1989**, *44B*, 263.

4. Date, A. R.; Hutchison, D. J. *Anal. At. Spectrom.* **1987**, *2*, 269.

5. Jarvis, K. E. *J. Anal. At. Spectrom.* **1989**, *4*, 563.

6. Shabani, M. B.; Masuda, A. *Anal. Chem.* **1991**, *63*, 2099.

7. Gregoire, D. C. *J. Anal. At. Spectrom.* **1988**, *3*, 309.

8. Date, A. R.; Gray, A. L. *Spectrochim. Acta* **1985**, *40B*, 115.

9. Date, A. R.; Hutchison, D. *Spectrochim. Acta* **1986**, *41B*, 175.

10. Park, C. J.; Hall, G. E. M. *J. Anal. At. Spectrom.* **1987**, *2*, 473.

11. Park, C. J.; Hall, G. E. M. *J. Anal. At. Spectrom.* **1988**, *3*, 355.

12. Date, A. R.; Stuart, M. E. *J. Anal. At. Spectrom.* **1988**, *3*, 659.

13. Jarvis, K. E.; Williams, J. G. *Chem. Geol.* **1989**, *77*, 53.

14. Jarvis, K. E. *Chem. Geol.* **1990**, *83*, 89.

15. Imai, N. *Anal. Chim. Acta* **1990**, *235*, 381.

16. Garbarino, J. R.; Taylor, H. E. *Anal. Chem.* **1987**, *59*, 1568.

17. Gregoire, D. C. *J. Anal. At. Spectrom.* **1990**, *5*, 623.

18. Ketterer, M. E. *Anal. Chem.* **1990**, *62*, 2522.

19. Date, A. R.; Cheung, Y. Y. *Analyst* **1987**, *112*, 1531.

20. Hirata, T.; Masuda, A. *J. Anal. At. Spectrom.* **1990**, *5*, 627.

21. Ward, D. B.; Bell, M. *Anal. Chim Acta* **1990**, *229*, 157.

22. Beauchemin, D.; Berman, S. S. *Anal. Chem.* **1989**, *61*, 1857.

23. Falkner, K. K.; Edmond, J. M. *Anal. Chem.* **1990**, *62*, 1477.

24. Klinkhammer, G. P.; Chan, L. H. *Anal. Chim. Acta* **1990**, *232*, 323.

25. Beauchemin, D.; McLaren, J. W.; Willie, S. N.; Berman, S. S. *Anal. Chem.* **1988**, *60*, 687.

26. Boomer, D. W.; Powell, M. J. *Anal. Chem.* **1987**, *59*, 2810.

27. Ting, B. T. G.; Janghorbani, M. *Anal. Chem.* **1986**, *58*, 1334.

28. Igarashi, Y.; Kawamura, H.; Shiraishi, K. *J. Anal. Atom. Spectrom.* **1989**, *4*, 571.

29. Viczian, M.; Lasztity, A.; Barnes, R. *J. Anal. Atom. Spectrom.* **1990**, *5*, 293.

30. Branch, S.; Ebdon, L.; Ford, M.; Foulkes, M.; O'Neill, P. *J. Anal. Atom. Spectrom.* **1991**, *6*, 151.

31. Thompson, J.; Ward, N. I. *J. Micronutr. Anal.* **1989**, *6*, 85.

32. Delves, H. T.; Campbell, M. J. *J. Anal. Atom. Spectrom.* **1988**, *3*, 343.

33. Gercken, B.; Barnes, R. M. *Anal. Chem.* **1991**, *63*, 1594.

34. Beck, G. L.; Farmer, O. T. *J. Anal. Atom. Spectrom.* **1988**, *3*, 771.

35. Peng, Z.; Klinkenberg, H.; Beeren, T.; Van Borm, W. *Spectrochim. Acta* **1991**, *46B*, 1051.

36. Zurhaar, A.; Mullings, L. *J. Anal. Atom. Spectrom.* **1990**, *5*, 611.

37. Gregoire, D. C. *Anal. Chem.* **1990**, *62*, 141.

38. Ward, D. B.; Bell, M. *Anal. Chim. Acta* **1990**, *229*, 157.

39. Shabani, M. B.; Akagi, T.; Masuda, A. *Anal. Chem.* **1993**, *64*, 737.

40. Houk, R. S.; Jiang, S. J. In *Trace Metal Analysis and Speciation*; (Ed.) Krull, I. S., Elsevier: Amsterdam, **1991**, Chapter 5.

41. Elder, R. C.; Jones, W. B.; Tepperman, K. In *Element-Specific Chromatographic Detection by Atomic Emission Spectroscopy*; (Ed.) Uden, P. C., ACS Symposium Series 479, Washington, DC, **1992**, Chapter 18.

42. Braverman, D. S. *J. Anal. At. Spectrom.* **1992**, *7*, 43.

43. Suyani, H.; Heitkemper, D.; Creed, J.; Caruso, J. A. *J. Appl. Spectrosc.* **1989**, *43*, 962.

44. Bushee, D. S. *Analyst* **1988**, *113*, 1167.

45. Bushee, D. S.; Moody, J. R.; May, J. C. *J. Anal. At. Spectrom.* **1989**, *4*, 773.

46. Thompson, J. J.; Houk, R. S. *Anal. Chem.* **1986**, *58*, 2541.

47. Jiang, S. J.; Houk, R. S. *Spectrochim. Acta, Part B*, **1988**, *43*, 405.

48. Beauchemin, D.; Siu, K. W. M.; McLaren, J. W.; Berman, S. S. *J. Anal. At. Spectrom.* **1989**, *4*, 285.

49. Shibata, Y.; Morita, M. *Anal. Chem.* **1989**, *61*, 2116.

50. Suyani, H.; Creed, J.; Davidson, T.; Caruso, J. A. *J. Chromatogr. Sci.* **1989**, *27*, 139.

51. Al-Rashdam, A.; Vela, N. P.; Caruso, J. A.; Heitkemper, K. T. *J. Anal. At. Spectrom.* **1992**, *7*, 551.

52. Shum, S. C. K.; Neddersen, R.; Houk, R. S. *Analyst* **1992**, *117*, 571.

53. Zhao, Z.; Jones, W. B.; Tepperman, K.; Dorsey, J. G.; Elder, R. C. *J. Pharm. Biomed. Anal.* **1992**, *10*, 279.

54. Shum, S. C. K.; Pang, H. M.; Houk, R. S. *Anal. Chem.* **1992**, *64*, 2444.

55. Sheppard, B. S.; Caruso, J. A.; Heitkemper, D. T.; Volnik, K. A. *Analyst* **1992**, *117*, 971.

56. Sheppard, B. S.; Shen, W. L.; Caruso, J. A.; Heikemper, D. T.; Fricke, F. L. *J. Anal. At. Spectrom.* **1990**, *5*, 431.

57. Heitkemper, D.; Creed, J.; Caruso J.; Fricke, F. L. *J. Anal. At. Spectrom.* **1989**, *4*, 279.

58. Suzuki, S.; Tsuchihashi, H.; Nakajima, K.; Matsushita, A.; Nagao, T. *J. Chromatogr.* **1988**, *437*, 322.

59. Kawabata, K.; Kishi, Y.; Kawaguchi, O.; Watanabe, Y.; Inoue, Y. *Anal. Chem.* **1991**, *63*, 2137.

60. Boomer, D. W.; Powell, J. J.; Hipfner, J. *Talanta* **1990**, *37*, 127.

61. Takatera, K.; Watanabe, T. *Anal. Sci.* **1992**, *8*, 469.

62. Owen, L. M. W.; Crews, H. M.; Hutton, R. C.; Walsh, A. *Analyst* **1992**, *117*, 649.

63. Gercken, B.; Barnes, R. M. *Anal. Chem.* **1991**, *63*, 283.

64. Takatera, K.; Watanabe, T. *Anal. Sci.* **1991**, *7*, 695.

65. Mason, A. Z.; Storms, S. D.; Jenkins, K. D. *Anal. Biochem.* **1990**, 186, 187.

66. Crews, H. M.; Dean, J. R.; Ebdon, L.; Massey, R. C. *Analyst* **1989**, 114, 895.

67. Matz, S. G.; Elder, R. C.; Tepperman, K. *J. Anal. At. Spectrom.* **1989**, *4*, 767.

68. Dean, J. R.; Munro, S.; Ebdon, L.; Crews, H. M.; Massey, R. C. *J. Anal. At. Spectrom.* **1987**, *2*, 607.

69. Shen, W. L.; Vela, N. P.; Sheppard, B. S.; Caruso, J. A. *Anal. Chem.* **1991**, *63*, 1491.

70. Van Loon, J. C.; Alcock, L. R.; Pinchin, W. H.; Frech, J. B. *Spectrosc. Letters* **1986**, *19*, 1125.

71. Chong, N. S.; Houk, R. S. *Appl. Spectrosc.* **1987**, *41*, 66.

72. Hasegawa, T.; Umemoto, M.; Haraguchi, H.; Hsiech, C.; Montaser, A. In *Inductively Coupled Plasmas in Analytical Atomic Spectrometry*, Second Edition; (Eds.) Montaser, A.; Golightly D. W., VCH Publishers: New York, **1992**, Chapter 8.

73. Crain, J. S.; Smith, F. G.; Houk, R. S. *Spectrochim. Acta* **1990**, *45B*, 249.

74. Wiederin, D. R.; Smith, F. G.; Houk, R. S. *Anal. Chem.* **1991**, *63*, 219.

75. Smith, F. G.; Wiederin, D. R.; Houk, R. S. submitted for publ. in *Anal. Chem.*

76. Houk, R. S., *Anal. Chem.* **1986**, *58*, 97A.

77. Houk, R. S.; Jiang, S. J. In *Trace Metal Analysis and Speciation*; (Ed.) Krull, I. S., Elsevier: New York, **1991**; Chapter 5.

78. Elder, R. C.; Jones, W. B.; Tepperman, K. In *Element-Specific Chromatographic Detection by Atomic Emission Spectrosopy*; (Ed.) Uden, P. C., ACS Symposium Series 479: Washington, DC, **1992**, Chapter 18.

79. Braverman, D. S. *J. Anal. At. Spectrom.* **1992**, *7*, 43.

80. Suyani, H.; Heitkemper, D.; Creed, J.; Caruso, *J. Appl. Spectrosc.* **1989**, *43*, 962.

81. Bushee, D. S. *Analyst* **1988**, *113*, 1167.

82. Bushee, D. S.; Moody, J. R.; May, J. C. *J. Anal. At. Spectrom.* **1989**, *4*, 773.

83. Thompson, J. J.; Houk, R. S. *Anal. Chem.* **1986**, *58*, 2541.

84. Jiang, S. J.; Houk, R. S. *Spectrochim. Acta* **1988**, *43B*, 405.

85. Beauchemin, D.; Siu, K. W. M.; McLaren, J. W.; Berman, S. S. *J. Anal At. Spectrom.* **1989**, *4*, 285.

86. Shibata, Y.; Morita, M. *Anal. Chem.* **1989**, *61*, 2116.

87. Suyani, H.; Creed, J.; Davidson, T.; Caruso, J. *J. Chromatogr. Sci.* **1989**, *27*, 139.

88. Al-Rashdan, A.; Vela, N. P.; Caruso, J. A.; Heitkemper, D. T. *J. Anal. At. Spectrom.* **1992**, *7*, 551.

89. Shum, S. C. K.; Neddersen, R.; Houk, R. S. *Analyst* **1992**, *117*, 577.

90. Zhao, Z.; Jones, W. B.; Tepperman, K.; Dorsey, J. G.; Elder, R. C. *J. Pharm. Biomed. Anal.* **1992**, *10*, 279.

91. Shum, S. C. K.; Pang, H. M.; Houk, R. S. *Anal. Chem.* **1992**, *64*, 2444.

92. Sheppard, B. S.; Caruso, J. A.; Heitkemper, D. T.; Wolnik, K. A. *Analyst* **1992**, *117*, 971.

93. Sheppard, B. S.; Shen, W. L.; Caruso, J. A.; Heitkemper, D. T.; Fricke, F. L. *J. Anal. At. Spectrom.* **1990**, *5*, 431.

94. Heitkemper, D.; Creed, J.; Caruso, J.; Fricke, F. L. *J. Anal. At. Spectrom.* **1989**, *4*, 279.

95. Suzuki, S.; Tsuchihashi, H.; Nakajima, K.; Matsushita, A.; Nagao, T. *J. Chromatogr.* **1988**, *437*, 322.

96. Kawabata, K.; Kishi, Y.; Kawaguchi, O.; Watanabe, Y.; Inoue, Y. *Anal. Chem.* **1991**, *63*, 2137.

97. Boomer, D. W.; Powell, M. J.; Hipfner, J. *Talanta* **1990**, *37*, 127.

98. Takatera, K.; Watanabe, T. *Anal. Sci.* **1992**, *8*, 469.

99. Owen, L. M. W.; Crews, H. M.; Hutton, R. C.; Walsh, A. *Analyst* **1992**, *117*, 649.

100. Gercken, B.; Barnes, R. A. *Anal. Chem.* **1991**, *63*, 283.

101. Takatera, K.; Watanabe, T. *Anal. Sci.* **1991**, *7*, 695.

102. Mason, A. Z.; Storms, S. K.; Jenkins, K. D. *Anal. Biochem.* **1990**, *186*, 187.

103. Crews, H. M.; Dean, J. R.; Ebdon, L.; Massey, R. C. *Analyst* **1989**, *114*, 895.

104. Matz, S. G.; Elder, R. C.; Tepperman, K. *J. Anal. At. Spectrom.* **1989**, *4*, 767.

105. Dean, J. R.; Munro, S.; Ebdon, L.; Crews, H. M.; Massey, R. C. *J. Anal. At. Spectrom.* **1987**, *2*, 607.

106. Pinset, J. *Biochem. J.*, **1954**, *57*, 10.

107. Schwarz, K.; Foltz, C. M. *J. Am. Chem. Soc.*, **1957**, *79*, 3292.

108. Byard, J. L., *Arch. Biochem. Biophys.* **1969**, *130*, 556.

109. Oyamada, N.; Ishizaki, M., *Jpn. J. Ind. Health* **1982**, *24*, 320.

110. Shamberger, R. J. Selenium, In *Biochemistry of the Essential Ultratrace Elements*; (Ed.) Frieden, E., Plenum Press: New York, **1984**, 201.

111. Florence, T. M. In *Trace Element Speciation: Analytical Methods and Problems*; (Ed.) Batley, G. E., CRC Press Inc.: Florida, **1989**, Chapter 9.

112. Underwood, E.J. In *Trace Elements in Human and Animal Nutrition*, Academic Press, New York, **1977**, 302.

113. Burk, R. F. *FASEB J.* **1991**, *5*, 2274.

114. Burk, R. F.; Lawrence, R. A.; Lane, J. M. *J. Clin. Invest.* **1980**, *65*, 1024.

115. Motsenbocker, M. A.; Tappel, A. L. *Biochim. Biophys. Acta* **1982**, *719*, 147.

116. Shum, S. Ph.D. Thesis, Iowa State University, **1993**.

117. LaFreniere, K. E.; Fassel, V. A.; Eckels, D. E. *Anal. Chem.* **1987**, *59*, 879.

118. Jarosz, J.; Mermet, J. M.; Robin, J. *C. R. Acad. Sci. Ser. B* **1974**, *27B*, 885.

119. Mermet, J. M. *Spectrochim. Acta* **1975**, *30B*, 383.

120. Jarosz, J.; Mermet, J. M. *J.Quant. Spectrosc. Radiat. Transfer* **1977**, *17*, 237.

121. Jarosz, J.; Mermet, J. M.; Robin, J. P. *Spectrochim. Acta* **1978**, *33B*, 55.

122. Abdallah, M. H.; Mermet, J. M. *J. Quant. Spectrosc. Radiat. Transfer* **1978**, *19*, 83.

123. Abdallah, M. H.; Mermet, J. M. *Spectrochim. Acta* **1982**, *37B*, 391.

124. Kalnicky, D. J.; Kniseley, R. N.; Fassel, V. A. *Spectrochim. Acta* **1975**, *30B*, 511.

125. Kalnicky, D. J.; Fassel, V. A.; Kniseley, R. N. *Appl. Spectrosc.* **1977**, *31*, 137.

126. Montaser, A.; Fassel, V. A.; Larsen, G. *Appl. Spectrosc.* **1981**, *35*, 385.

127. Kornblum, G. R.; De Galan, L. *Spectrochim. Acta* **1974**, *29B*, 249.

128. Kornblum, G. R.; De Galan, L. *Spectrochim. Acta* **1977**, *32B*, 71.

129. Furuta, N.; Horlick, G. *Spectrochim. Acta* **1982**, *37B*, 53.

130. Alder, J. F.; Bombelka, R. M.; Kirkbright, G. F. *Spectrochim. Acta* **1980**, *35B*, 163.

131. Uchida, H. J.; Tanabe, K.; Nojri, Y.; Haraguchi, H.; Fuwa, K. *Spectrochim. Acta* **1981**, *36B*, 711.

132. Kawaguchi, H.; Ito, T.; Mizuike, A. *Spectrochim. Acta* **1981**, *36B*, 615.

133. Gunter, W. H.; Visser, K.; Zeeman, P. B. *Spectrochim. Acta* **1983**, *38B*, 949.

134. Faires, L. M.; Palmer, B. A.; Engleman, R.; Niemczyk, T. M. *Spectrochim. Acta* **1984** *39B*, 819.

135. Blades, M. W.; Caughlin, B. L. *Spectrochim. Acta* **1985**, *40B*, 579.

136. Caughlin, B. L.; Blades, M. W. *Spectrochim. Acta* **1985**, *40B*, 987.

137. Capelle, B.; Mermet, J. M.; Robin, J. *Appl. Spectrosc.* **1982**, *36*, 102.

138. Furuta, N.; Nojiri, N.; Fuwa, K. *Spectrochim. Acta* **1985**, *40B*, 423.

139. Caughlin, B. L.; Blades, M. W. *Spectrochim. Acta* **1984**, *39B*, 1583.

140. Caughlin, B. L.; Blades, M. W. *Spectrochim. Acta* **1985**, *40B*, 1539.

141. Boumans, P. W. J. M. *Excitation Spectra in Analytical Emission Spectrometry*; (Ed.) Grove, E. L., Dekker: New York, **1972**.

142. Thorne, A. P. *Spectrophysics*, Chapmin & Hall: London, **1974**.

143. Walker, Z.; Blades, M. W. *Spectrochim. Acta* **1986**, *41B*, 761.

144. Smith, F. G. Ph.D. Thesis, Iowa State University, **1991**.

145. Cremers, C. J.; Birkebak, R. C. *Applied Optics* **1966**, *5*, 1057.

146. Bridges, J. M.; Kornblith, R. L. *Astrophys.* **1974**, *192*, 793.

147. Moity *Astron. Astrophys. Suppl. Ser.* **1983**, *52*, 37.

148. Whaling, W. *Technical Report 84A*, Kellog Radiation Laboratory, California Institute of Technology, **1985**.

149. Tamaki, S.; Kuroda, T. *Spectrochimica Acta* **1987**, *42B*, 1105.

150. Ishii, I.; Montaser, A. *Spectrochim. Acta* **1991**, *46B*, 1197.

151. Hasegawa, T.; Umemoto, M.; Haraguchi, H.; Hsiech, C.; Montaser, A. In *Inductively Coupled Plasmas in Analytical Atomic Spectrometry* Second Edition; (Ed.) Montaser, A.; Golightly, D. W., VCH Publishers, Inc.: New York, **1992**, Chapter 8.

152. Moore, C. E. *Atomic Energy Levels Vol. II*, Circular 467, United States Department of Commerce, NBS, **1952**.

153. Robin, J. P. *Prog. Anal. Atom. Spectrosc.* **1982**, *5*, 79.

154. Goldwasser, A.; Mermet, J. M. *Spectrochim. Acta* **1986**, *41B*, 725.

155. Farnsworth, P. B.; Smith, B. W.; Omenetto, N. *Spectrochim. Acta* **1991**, *46B*, 843.

ACKNOWLEDGMENTS

I would first like to thank Dr. Houk for allowing and helping me to learn and do research in his lab. I would also like to thank all the Houk Group members, past and present. Each one has helped me at sometime during my stay in Ames. They have not only been helpful in the laboratory but have made my stay in Ames more enjoyable. I'd also like to thank all my friends in Ames, both in the Chemistry department and those I was fortunate enough to meet outside the department. Many people have asked me, and probably more will, the following question: Don't you think it was a waste to spend three years here and then not want a job in chemistry? Part of the reason I answer no to this question is because of all the people I have met here. Of course, another is you never know what might happen. I learned a lot in the past three years about chemistry, among other things, including myself. I will never look back on this time and think of it as a waste. It is a part of my life and together with the rest it makes me who I am. I would like to give a special thanks to Dr. Houk for allowing me to take some time away and then to return to graduate school after my trip to India. The trip taught me so much and helped me regain perspective in my life. Travel is an important educator; it opens the eyes and the heart to many things and also, to gifts we should appreciate while on this planet earth. Thank you to my family, especially my mom, for always loving me and being proud of me for whatever I choose to do. Finally, I'd like to thank the One Above for always guiding me throughout my life, and for all the joy and beauty around me.

This work was performed at Ames Laboratory under Contract No. W-7405-eng-82 with the U.S. Department of Energy. The United States government has assigned the DOE Report number IS-T1701 to this thesis.